

UNCLASSIFIED

AD NUMBER	
AD323599	
CLASSIFICATION CHANGES	
TO:	UNCLASSIFIED
FROM:	CONFIDENTIAL
LIMITATION CHANGES	
TO:	Approved for public release; distribution is unlimited. Document partially illegible.
FROM:	Distribution authorized to U.S. Gov't. agencies and their contractors; Administrative/Operational Use; 13 FEB 1961. Other requests shall be referred to Army Dugway Proving Ground, UT 84022. Document partially illegible.
AUTHORITY	
OSD/WHS ltr dtd 1 Aug 2013; OSD/WHS ltr dtd 1 Aug 2013	

THIS PAGE IS UNCLASSIFIED

#11

Page determined to be Unclassified
Reviewed Chief, RDD, WHS
IAW EO 13526, Section 3.6
Date: **MAY 17 2013**

~~AD- 32359~~
SECURITY REMARKING REQUIREMENTS
~~DOD 5200.1-R, DEC 78~~
~~REVIEW ON 28 FEB 81~~

Office of the Secretary of Defense *SVSCS552*
Chief, RDD, ESD, WHS
Date: 17 MAY 2013 Authority: EO 13526
Declassify: X Deny in Full: _____
Declassify in Part: _____
Reason: _____
MDR: 12-M-3154

12-M-3154 R-1

~~CONFIDENTIAL~~

AD **323 599**

*Reproduced
by the*

ARMED SERVICES TECHNICAL INFORMATION AGENCY
ARLINGTON HALL STATION
ARLINGTON 12, VIRGINIA



~~CONFIDENTIAL~~

DECLASSIFIED IN FULL
Authority: EO 13526
Chief, Records & Declass Div, WHS
Date: MAY 17 2013

NOTICE: When government or other drawings, specifications or other data are used for any purpose other than in connection with a definitely related government procurement operation, the U. S. Government thereby incurs no responsibility, nor any obligation whatsoever; and the fact that the Government may have formulated, furnished, or in any way supplied the said drawings, specifications, or other data is not to be regarded by implication or otherwise as in any manner licensing the holder or any other person or corporation, or conveying any rights or permission to manufacture, use or sell any patented invention that may in any way be related thereto.

Page determined to be Unclassified

Reviewed Chief, RDD, WHS

IAW EO 13526, Section 3.5

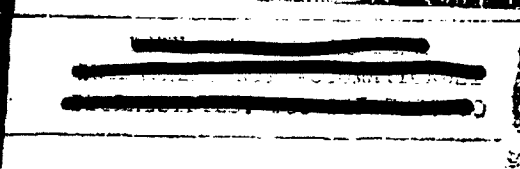
Date: MAY 17 2013

CATALOGED BY ASTIA
AS AD No.

323599

DECLASSIFIED IN FULL
Authority: EO 13526
Chief, Records & Declass Div, WHS
Date: MAY 17 2013

MECHANICAL DIVISION



TO WIDE WORLD THROUGH INTENSIVE RESEARCH • CREATIVE ENGINEERING • PRECISION MANUFACTURING

~~CONFIDENTIAL~~

This document consists of 10 pages and is number 1 of 10 copies, series C, and the following attachments.

COPY

Mechanical Division of
GENERAL MILLS, INC.
Research Department
2003 East Hennepin Avenue
Minneapolis 13, Minnesota

3559⁰

SECOND QUARTERLY PROGRESS REPORT
ON
DISSEMINATION OF SOLID
AND LIQUID BW AGENTS
(Unclassified Title)

XEROX

For Period: 4 September - 4 December, 1960

ASTIA
REF ID: A
JUN 13 1961
TIPDR

Contract No. DA-18-064-CML-2745

Prepared for

S. Army Biological Warfare Laboratories
Fort Detrick
Frederick, Maryland

COPY

Submitted by:

G. R. Whitnah
G. R. Whitnah
Project Manager

Approved by:

S. P. Jones
S. P. Jones, Manager
Materials & Mechanics Research

Report No. 2161
Project No. 82408
Date: February 13, 1961

~~CONFIDENTIAL~~
~~NOT AUTOMATED~~
DOD DIR 5200.10

~~CONFIDENTIAL~~

DECLASSIFIED IN FULL
Authority: EO 13526
Chief, Records & Declass Div, WHS
Date: MAY 17 2013

~~CONFIDENTIAL~~

ABSTRACT

This Second Quarterly Progress Report covers research on dissemination of solid and liquid BW agents. The objective toward which this research is directed is the development of weapon systems for the dissemination of these agents as a line source from high speed low-flying manned and unmanned aircraft.

The results of experiments on feeding of finely divided solid materials with helical screws and piston devices are presented.

Experiments on dissemination and deagglomeration are described. These include preliminary investigations of aerosol generation by erosion and also with a liquid carbon dioxide system. Deagglomeration experiments in a high-subsonic wind tunnel are described.

Results of studies of the characteristics of finely divided materials are given. These studies include a literature search, theoretical investigations and experiments.

Aerodynamic data for wing-mounted external stores are presented. The effects of the external geometry and the pylon design on the incremental drag coefficients are discussed.

The status of design studies on a research prototype of a liquid agent disseminating store which is covered in a separate report is briefly outlined.

DECLASSIFIED IN FULL
Authority: EO 13526
Chief, Records & Declass Div, WHS
Date:

MAY 17 2013

~~CONFIDENTIAL~~

Foreword

Members of the Research Department Staff who have participated in directing and conducting the investigations and preparing the discussions presented in this report include Messrs. S. P. Jones, Jr., G. Whitnah, A. Anderson, W. L. Torgeson, J. Upton, C. Hagberg, P. Stroom, G. Morfitt, R. Griffith, I. Hall, J. Pilney, R. Dahlberg and G. Uhngs.

DECLASSIFIED IN FULL
Authority: EO 13526
Chief, Records & Declass Div, WHS
Date:

MAY 17 2013

~~CONFIDENTIAL~~

~~CONFIDENTIAL~~
TABLE OF CONTENTS

<u>Section</u>		<u>Page</u>
ABSTRACT		ii
FOREWORD		iii
1. INTRODUCTION		1
2. EXPERIMENTS ON FEEDING DRY POWDERS		2
2.1. Experiments With Screw Feeders		2
2.1.1 Description of Apparatus		3
2.1.2 General Procedure		5
2.1.3 Experiments With SM Simulant		5
2.1.4 Experiments With Talc		12
2.1.5 Summary		12
2.2 Experiments on Piston Feeding		14
3. DISSEMINATION AND DEAGGLOMERATION EXPERIMENTS		17
3.1 Investigations of Erosion as a Method of Dissemination of Finely Divided Materials		17
3.1.1 Initial Experiment		17
3.1.2 Erosion Experiments With Talc		20
3.2 Experiments on the Use of Carbon Dioxide to Disperse Finely Divided Solids		27
3.3 High Velocity Sampling Probe Tests		29
3.4 Deagglomeration Experiments		35
3.4.1 Apparatus		35
3.4.2 Preliminary Experiments		35

DECLASSIFIED IN FULL
Authority: EO 13526
Chief, Records & Declass Div, WHS
Date: **MAY 17 2013**

~~CONFIDENTIAL~~

TABLE OF CONTENTS (Continued)

<u>Section</u>		<u>Page</u>
4.	INVESTIGATIONS OF THE CHARACTERISTICS OF FINELY DIVIDED MATERIALS	42
4.1	Literature Search	42
4.1.1	Specific Surface Area	42
4.1.2	Relation of Size Distribution to Plasticity, Dilatancy and Force Transmission in Bulk Powder	43
4.2	Theoretical Investigation	46
4.2.1	Analysis of Static Load Transmission in Granular Packings	47
4.2.2	Static Load Transmission in Regular Packings	49
4.2.2.1	Square Arrays	49
4.2.2.2	Hexagonal Arrays	49
4.3	Experiments on Characteristics of Powders	56
4.3.1	Translation of Particles Above a Moving Piston	56
4.3.2	Gravity Flow of Particles	58
4.3.3	Torque Required to Rotate a Helical Screw Configuration in a Powder Bed	59
4.4	Experimental Particle Size Analysis	60
4.4.1	Centrifuge Operating Principle	60
4.4.2	Results	62
5.	STUDIES OF THE AERODYNAMIC CHARACTERISTICS OF WING-MOUNTED EXTERNAL AIRCRAFT STORES	69
5.1	Installed External Store Data	69
5.2	Discussion of Aerodynamic Data	78
6.	INVESTIGATION OF PROPERTIES OF SLURRIES	81
6.1	Properties of Egg Slurries	81

~~CONFIDENTIAL~~

Y
DECLASSIFIED IN FULL
Authority: EO 13526
Chief, Records & Declass Div, WHS
Date:

MAY 17 2013

~~CONFIDENTIAL~~

TABLE OF CONTENTS (Continued)

Section	Page
6.2 Properties of Slurries of SM in Inert Fluorochemical Liquid	84
7. WORK ON LIQUID AGENT DISSEMINATORS	87
8. SUMMARY AND CONCLUSIONS	88

APPENDIX A

PROCEDURE FOR CALCULATION OF TIME SCHEDULES FOR WHITBY CENTRIFUGE PARTICLE SIZE ANALYSIS TECHNIQUE

1. Gravity Sedimentation Period	A-1
2. Centrifuge Operating Period	A-2

DECLASSIFIED IN FULL
Authority: EO 13526
Chief, Records & Declass Div, WHS
Date: MAY 17 2013

~~CONFIDENTIAL~~

~~CONFIDENTIAL~~

LIST OF ILLUSTRATIONS

<u>Figure</u>		<u>Page</u>
2.1.1	Experimental Screw-Feeding Device	4
2.1.2	Delivery Characteristics of Closed-Center Helical Screw, Filled With SM at 50% Atmospheric Relative Humidity	7
2.1.3	Delivery Characteristics of Closed-Center Helical Screw, Filled With SM at 15% Atmospheric Relative Humidity	8
2.1.4	Delivery Characteristics of Closed-Center Helical Screw, Filled With SM at 5% Atmospheric Relative Humidity	9
2.1.5	Delivery Characteristics of Open-Center Helical Screw, Filled With SM at 15% Atmospheric Relative Humidity	11
2.2.1	Characteristics of Piston Feeding Device, Filled With Sierra Mistron No. 18 Talc.	15
3.1.1	Results of Initial Experiment With Flour	19
3.1.2	Typical Photographs of Aerosol Clouds Generated by Erosion	21
3.1.3	Average Mass Flow Rate Versus Time for Erosion Type Aerosol Generator (Model 2)	23
3.1.4	Average Mass Flow Rate Versus Time for Erosion Type Aerosol Generator (Model No. 3)	26
3.3.1	Pressure Ratio Versus Mass Flow Ratio for High Velocity Sampling Probe	31
3.3.2	Diffuser Efficiency Versus Mass Flow Ratio for High Velocity Sampling Probe	33
3.4.1	Piston-Type Feeding Device	36
3.4.2	Feeding Device Mounted on Top of Wind Tunnel Test Section . . .	37
3.4.3	Microphotograph (600X) of Flour Before Dissemination	39
3.4.4	Microphotograph (600X) of Flour After Dissemination	39
4.2.1	Vertical Square Array	50

DECLASSIFIED IN FULL
 Authority: EO 13526
 Chief, Records & Declass Div, WHS
 Date: MAY 17 2013

~~CONFIDENTIAL~~

~~CONFIDENTIAL~~

LIST OF ILLUSTRATIONS (Continued)

<u>Figure</u>	<u>Page</u>
4.2.2 45° Square Array	50
4.2.3 Hexagonal Array - Configuration I	51
4.2.4 Hexagonal Array - Configuration II	51
4.3.1 Apparatus for Studying Translation of Particles Above a Moving Piston	57
4.4.1 Duplicate Size Analyses on SM Sample GBL#B-0807006	63
4.4.2 Duplicate Size Analyses on SM Sample GBL#A-3416554	64
4.4.3 Duplicate Size Analyses on SM Sample GBL#A-3416691	65
4.4.4 Centrifuge Size Distribution for Talc	66
4.4.5 Centrifuge Size Analysis for GMI "Jet" Flour	67
5.1.1 Ordinates, in Percent Length, for Five NACA 65A-Series Bodies of Revolution Used as External Stores	71
5.1.2 Incremental Drag Coefficient Versus Flight Mach Number for Various External Store Configurations at Zero Lift Coefficient	74
5.1.3 Incremental Drag Coefficient Versus Flight Mach Number for Various External Store Configurations at Lift Coefficient (C_L) of 0.3	75
5.2.1 Shape Definition, Subsonic External Store	79
6.1.1 Shear Rate Versus Shear Stress for Egg Slurry Samples at 20°C	83
6.2.1 Effect of Variation in Shear Rate on the Apparent Viscosity of Slurries of SM in Fluorochemical Liquid FC-75	85

APPENDIX A

A-1 Typical Starting and Stopping Curves	A-4
--	-----

DECLASSIFIED IN FULL
 Authority: EO 13526
 Chief, Records & Declass Div, WHS
 Date: MAY 17 2013

~~CONFIDENTIAL~~

~~CONFIDENTIAL~~

1. INTRODUCTION

This is the Second Quarterly Progress Report on the program of research on dissemination of solid and liquid BW agents being conducted under Contract No. DA-18-064-CML-2745. The research work is directed toward the development of external airborne disseminating stores for use on low altitude delivery vehicles, operating in the speed range of 0.70 to 0.90 Mach Number.

Since both solid and liquid agents are considered in the scope of this project, the subjects discussed in this report cover a wide range of technical fields. In presenting the progress in each of these areas, we have tried to show the relationship of the individual areas to the total project.

The major fields of study during this quarter include feeding and handling of finely divided dry materials, dissemination and deagglomeration, characteristics of finely divided solids, and aerodynamic characteristics of external aircraft stores.

The progress on the design studies on a research prototype of a liquid agent disseminating store is very briefly summarized. This part of the work is covered in detail in a separate report.^{1.1}

1.1 North American Aviation, Inc., Report No. NA-60-1403 Submitted to General Mills, Inc., November 15, 1960 (SECRET)

DECLASSIFIED IN FULL
Authority: EO 13526
Chief, Records & Declass Div, WHS
Date: MAY 17 2013

~~CONFIDENTIAL~~

~~CONFIDENTIAL~~

2. EXPERIMENTS ON FEEDING DRY POWDERS

2.1 Experiments with Screw Feeders

The possibility of employing screw feeding systems in the design of external stores for dissemination of solid BW agents was discussed in our first progress report. 2.1.1 Two illustrative configurations were described, one employing a large helical screw which occupied the full diameter and length of the agent storage chamber, so that the problem of feeding material to the screw was eliminated; the other employing a small screw feeder at the bottom of the agent chamber, with a system of rotating rods to prevent bridging of the material.

The experiments which are described herein were made to explore the characteristics of the first configuration: the large screw which receives no additional particulate material after it has been initially filled. Two potential problems mentioned in Reference 2.1.1 were (1) the possibility that the particulate material in the screw might rotate with the screw as a solid slug, because the friction at the wall of the enclosing cylinder was not great enough to cause relative motion between the agent and the screw, and (2) the possibility that a small clearance between the screw and the wall might be required for efficient operation, and that this restriction on clearance might cause serious problems in the design and manufacture of a flexible structure of this type.

2.1.1 General Mills, Inc., Report No. 2125 "Dissemination of Solid and Liquid BW Agents" (Unclassified Title) October 13, 1960, (SECRET)
p. 9

~~CONFIDENTIAL~~

~~CONFIDENTIAL~~

As a result of the series of experiments described below, it appears that neither of these potential problems are serious. The particulate material did not rotate as a solid slug in any of the cases investigated. Experiments with relatively small and large clearances showed that there was no serious effect of the large clearance.

2.1.1 Description of Apparatus

The screw feeding apparatus used in these experiments is shown in Figure 2.1.1. Two screw configurations were used. The first was a helical screw with a solid center section, and the second was a helical "ribbon type" screw with an open center section. Both of these screws were 44 mm in diameter and 230 mm long with a pitch of 51 mm. The diameter of the solid central shaft of the first screw was 22 mm, and the width of the ribbon on the screw with the open center section was 11 mm.

The clearance between the screw and the inner surface of the cylindrical lucite enclosure was 3.5 mm. A special glass sleeve was also made which had an internal diameter of 46 mm, leaving only 1 mm clearance around the screw when it was inserted into the lucite cylinder. This arrangement made it possible to investigate the effects of a substantial change in clearance with a minimum of alteration of the apparatus.

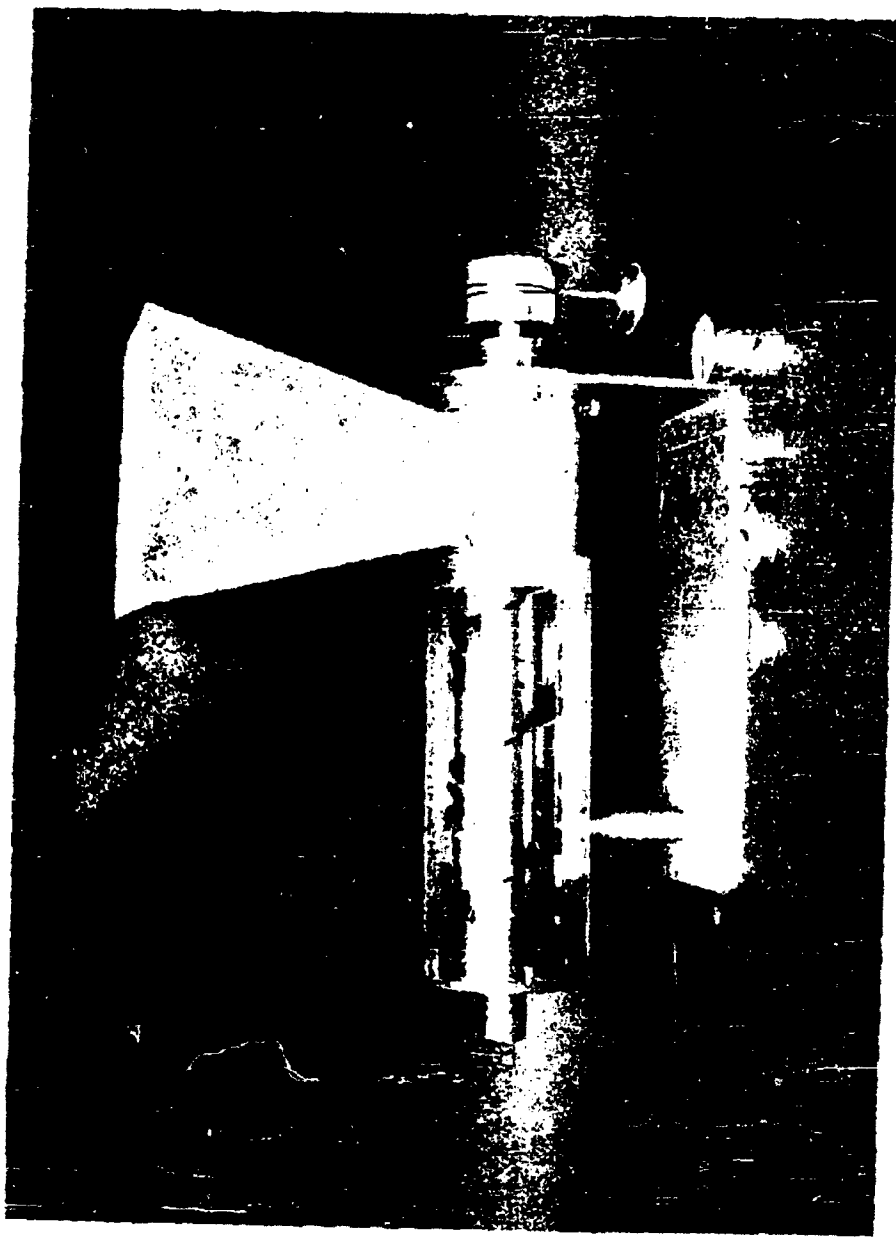
The discharge end of the apparatus was open except for a narrow spider to support the end bearing. The diameter of this opening was equal to the internal diameter of the lucite cylinder. The feeding hopper which is shown in Figure 2.1.1 was only used during the process of initially filling the screw. The experiments were all started with particulate material only in the cylindrical part of the apparatus, and no material was added.

DECLASSIFIED IN FULL

Authority: EO 13526
Chief, Records & Declass Div, WHS
Date:

MAY 17 2013

~~CONFIDENTIAL~~



Page determined to be Unclassified
Reviewed Chief, RDD, WHS
IAW EO 13526, Section 3.5
Date: MAY 17 2013

~~CONFIDENTIAL~~

2.1.2 General Procedure

In this series of experiments the cylindrical section of the apparatus was filled with a measured mass of the selected particulate material. This was done by temporarily sealing off the discharge end and rotating the screw by hand. A small electric vibrator was held in contact with the center shaft to improve the distribution in the screw.

After the discharge had been opened, the procedure was to collect and weigh the quantity of material discharged for a recorded angular rotation of the shaft. A knife blade was used to remove material protruding beyond the vertical plane of the discharge opening.

The early experiments were made by weighing the material discharged after every revolution, and the resulting data showed a nearly linear decline in quantity discharged per revolution as a function of the total revolutions from the start. However, further measurements of the discharge per half revolution revealed a considerable variation in discharge rate between these smaller rotational increments. The technique of measuring discharge every half revolution was therefore used throughout the series of experiments.

2.1.3 Experiments with SM Simulant

A series of experiments on the feeding characteristics of the above described screw configurations were made using SM simulant. These measurements were made with the feeding apparatus in a controlled humidity chamber. The effect of humidity on the characteristics of the helical screw with the solid center section was evaluated at relative humidity values of 5, 15 and 50 percent. The SM was placed in an open flat container in the controlled humidity chamber approximately 16 hours before each experiment was started.

DECLASSIFIED IN FULL

Authority: EO 13526

Chief, Records & Declass Div, WHS

Date:

MAY 17 2013

~~CONFIDENTIAL~~

~~CONFIDENTIAL~~

The material discharge rate (gm/1/2 revolution) was measured as a function of the total revolutions from the starting position. Each case was repeated three times, to explore the reproducibility of the process.

The results of these experiments are summarized in Figures 2.1.2, 2.1.3 and 2.1.4. Pertinent information on the conditions of the test are given on each graph. All of these tests were conducted with samples of SM taken from the lot designated as GBL-A-3416554, which is the number of the Government Bill of Lading identifying the shipments received from Fort Detrick. The particle size analyses performed on these samples are discussed in Section 4.4, of this report.

The experiments covered by Figures 2.1.2 through 2.1.4 were made with the glass sleeve (described in Section 2.1.1) in place, so that the clearance between the screw and the enclosure was 1.0 mm.

Examination of Figure 2.1.2 shows that (at 50% RH) the discharge rate decreases as a function of the total revolutions from start, and approached zero at about 10 revolutions. In these experiments, approximately 95 percent of the material originally loaded into the screw was discharged. The fact that this high percentage of the original material was reliably discharged by turning the screw through ten revolutions suggests that this feeding technique deserves consideration.

In order to provide a constant feed rate versus time, the rotational speed of the screw could be programmed to compensate for the natural characteristic. The high rate of discharge in the first half-revolution is a result of the geometry of the end of the screw. It appears that this could be

DECLASSIFIED IN FULL
Authority: EO 13526
Chief, Records & Declass Div, WHS
Date: MAY 17 2013

~~CONFIDENTIAL~~

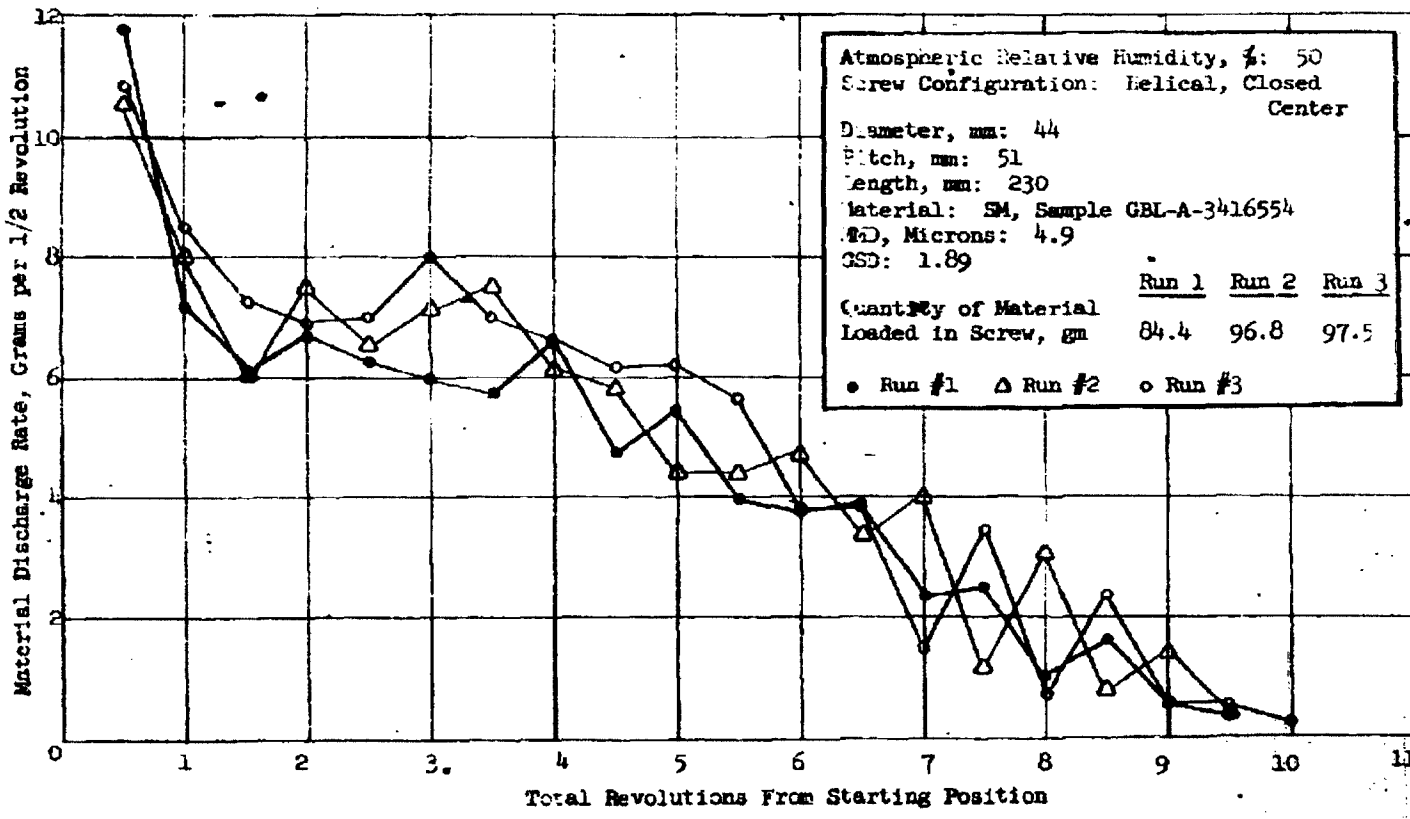


Figure 2.1.2 Delivery Characteristics of Closed-Center Helical Screw,
Filled with SM at 50% Atmospheric Relative Humidity

- 7 -

Page determined to be Unclassified
Reviewed Chief, RDD:WHS
IAW EO 13526, Section 3.5

Date: MAY 17 2013

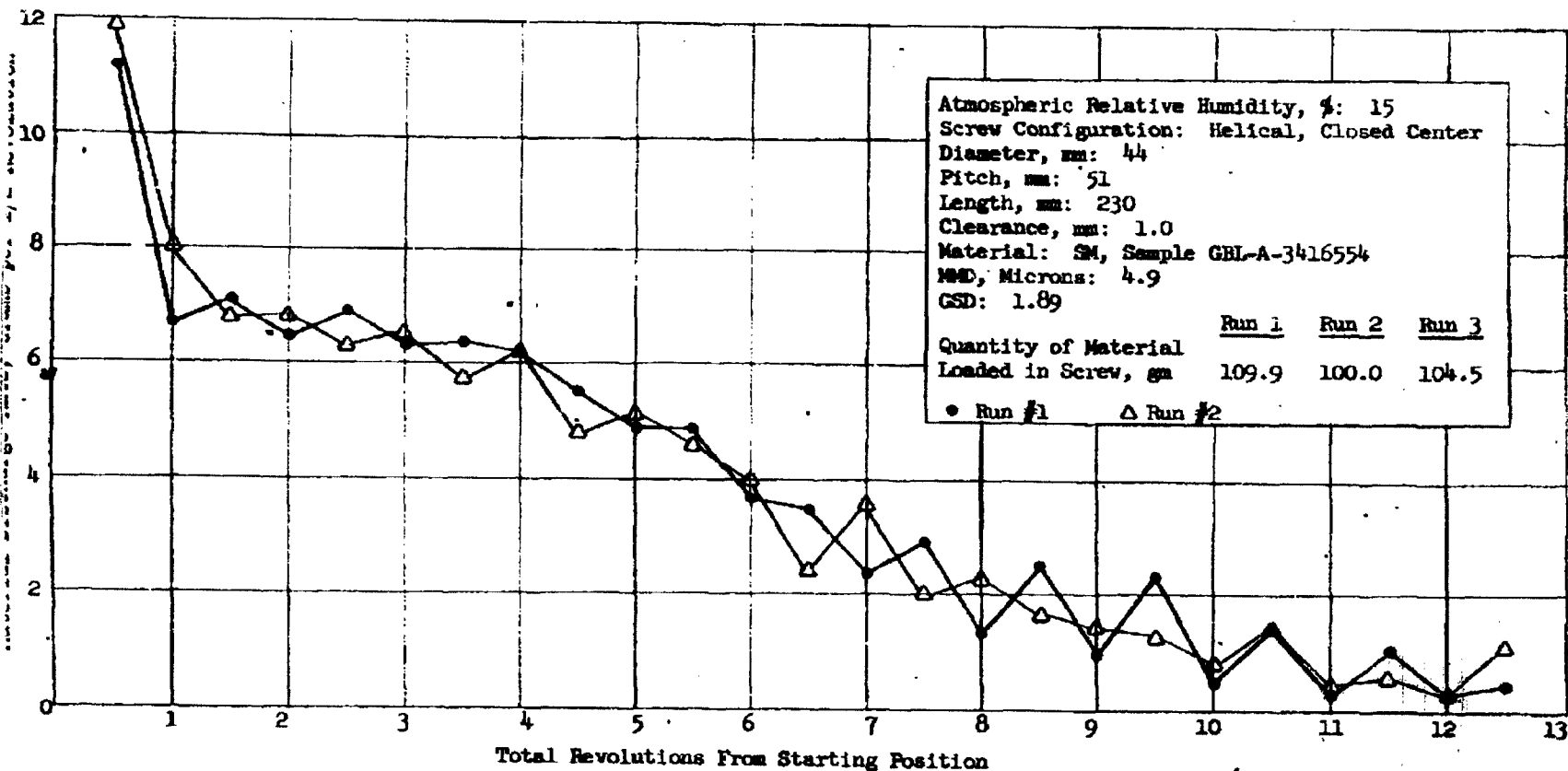


Figure 2.1.3 Delivery Characteristics of Closed-Center Helical Screw,
 Filled with SM at 15% Atmospheric Relative Humidity

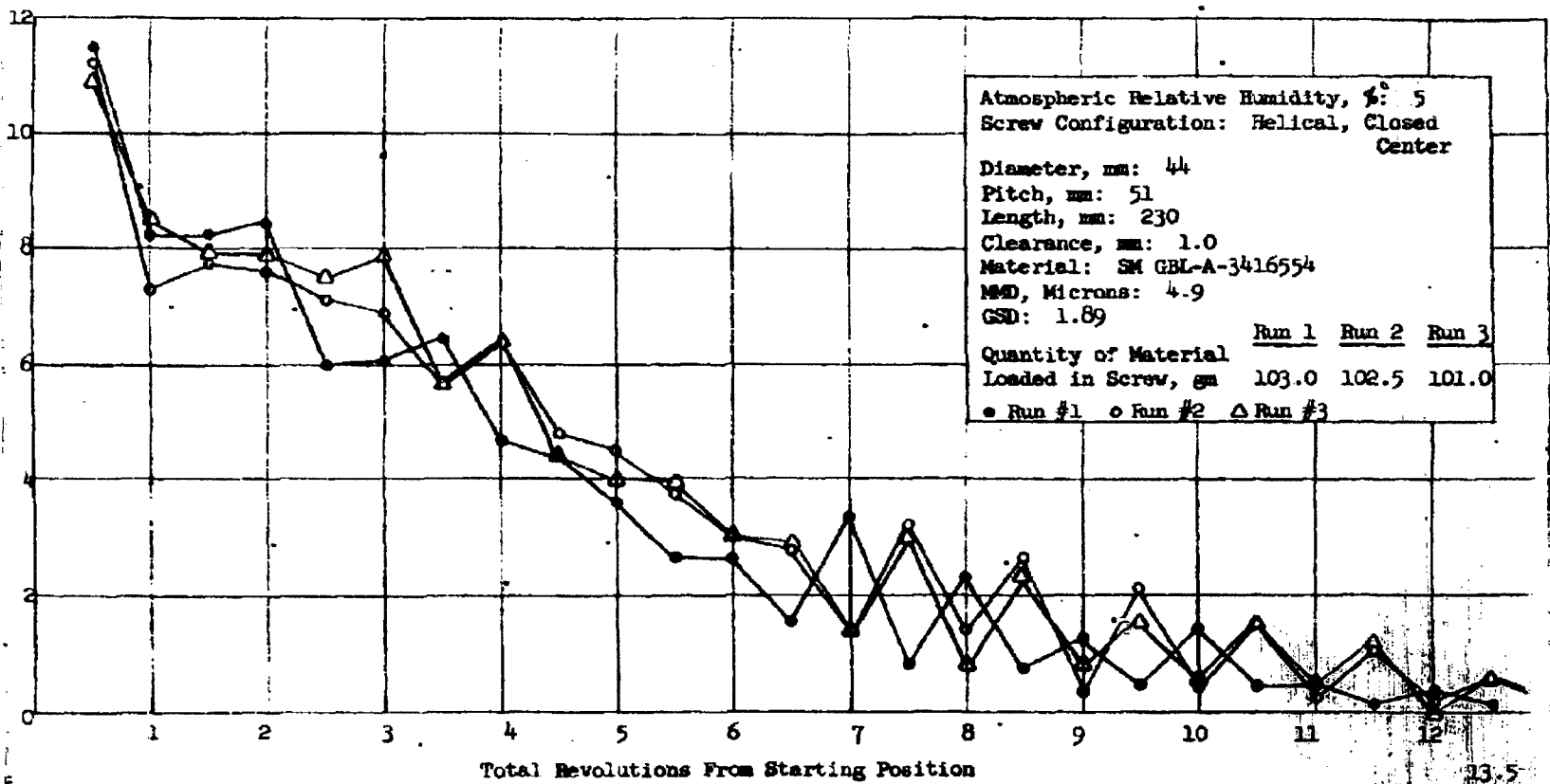


Figure 2.1.4 Delivery Characteristics of Closed-Center Helical Screw,
 Filled with SM at 5% Atmospheric Relative Humidity

Page determined to be Unclassified
 Reviewed Chief, RDD, WHS
 IAW EO 13526, Section 3.5
 Date: MAY 17 2013

~~CONFIDENTIAL~~

modified if a more nearly linear characteristic was desired. The graph shows considerable fluctuation in the feed rate, particularly towards the end of the process. If this device were employed in a disseminating store, it appears that the final metering and deagglomeration compartment would have to be capable of smoothing out this surging tendency.

Figure 2.1.3 shows the performance of this device when the relative humidity in the chamber was reduced to 15%. The results are very similar, with the exception that small quantities of material were being delivered after 12 revolutions in contrast to the process in Figure 2.1.2 which was complete in 10 revolutions. In the experiments of Figure 2.1.3, approximately 94 percent of the original material was discharged.

Figure 2.1.4 gives similar information for experiments conducted at 5 percent relative humidity. Rather important changes were observed in this case. The material appeared to be highly charged, and adhered to the metal rotor. The total quantity of material discharged varied considerably. The percentage of the material which was discharged in Runs 1, 2 and 3, were respectively, 79, 94 and 91 percent. These numbers are lower than the previously described cases, due to residual material adhering to the screw. It should be mentioned, however, that a substantial fraction of the residual material was located on the rather large center shaft. This effect might be insignificant for a ribbon-type screw.

The characteristics of the ribbon-type screw with an open center section are shown in Figure 2.1.5. The results are quite similar to those discussed previously. However, it should be noted that the numerical values

~~CONFIDENTIAL~~

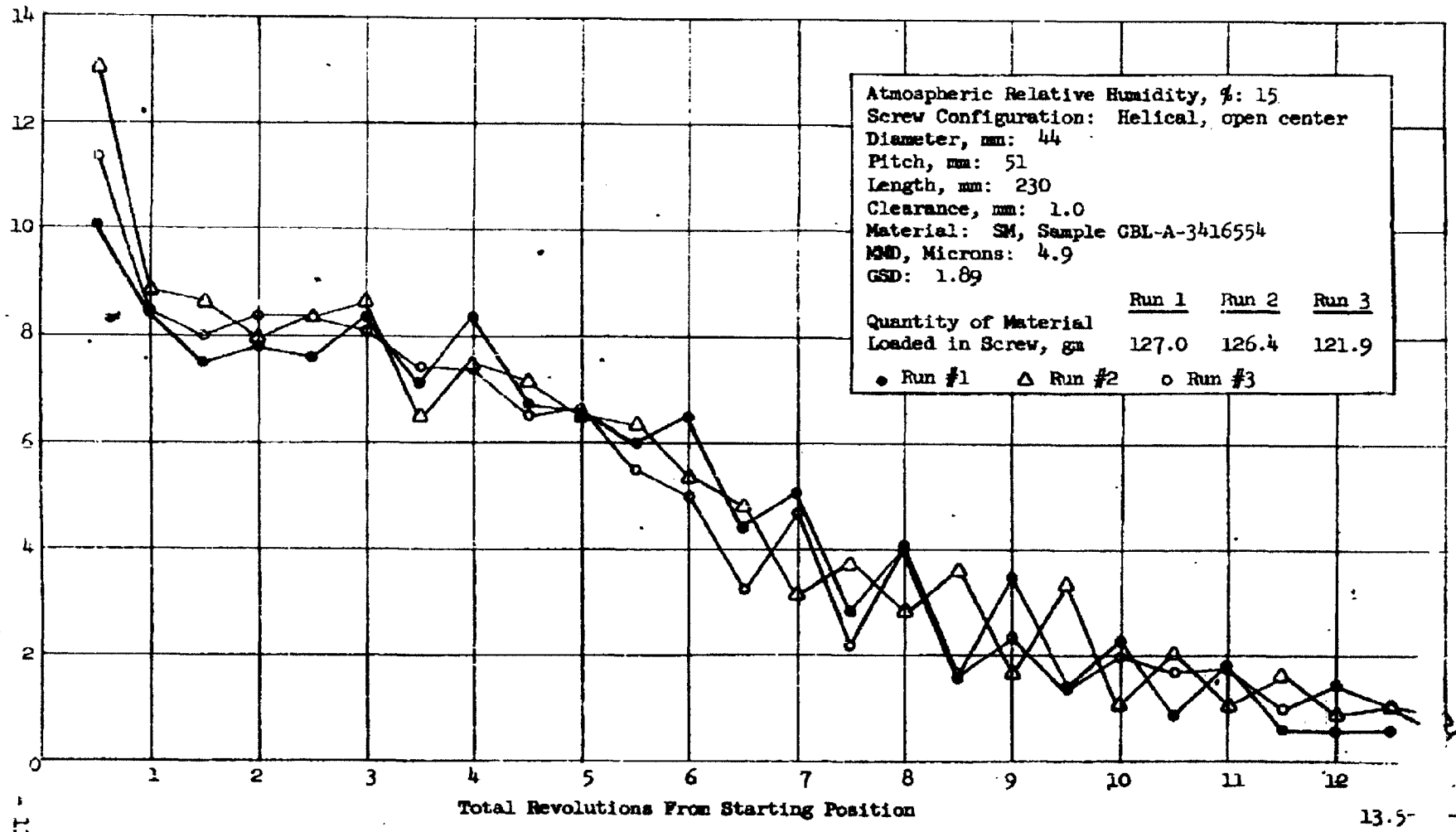


Figure 2.1.5 Delivery Characteristics of Open-Center Helical Screw,
Filled with SM at 15% Atmospheric Relative Humidity

~~CONFIDENTIAL~~

of the discharge rate are substantially higher than for the solid-center screw, reflecting the increase (about 25%) in total capacity for particulate material. The performance was better in every respect, and 95 to 99 percent of the material was discharged in 13 to 13.5 revolutions.

2.1.4 Experiments with Talc

Several measurements of the performance of these screw feeders were made with Sierra Mistron #18 talc. The results are very similar to the results presented above for SM, and are therefore not shown in detail.

In these experiments with talc, we also investigated the effect of additional clearance around the screw. With the glass sleeve removed from the apparatus, the clearance was increased to 3.5 mm. The main effect of this change was to increase the residual material. The friction between the particles and the wall was sufficient to stop the material in the lower parts of the clearance space from being advanced by the screw. This configuration delivered approximately 80 percent of the material originally placed in the apparatus. This reduction in delivery is rather substantial, but should be considered in light of the fact that the clearance was 16 percent of the radius of the screw. It does not appear that there would be any incentive to design a feeding system with a clearance of this magnitude.

2.1.5 Summary

These experiments with the ribbon-type and closed-center screw configurations show that, for the rather limited cases investigated, the device reliably delivers a high percentage of its contained particulate material.

DECLASSIFIED IN FULL
Authority: EO 13526
Chief, Records & Declass Div, WHS
Date: MAY 17 2013

~~CONFIDENTIAL~~

~~CONFIDENTIAL~~

This was accomplished in 10 to 13.5 revolutions from the starting position. No tendency to lock or bind was observed.

When the device was filled with SM which had been stored in a controlled atmosphere at 5% relative humidity for 16 hours, some effects of electrostatic charging were noted. In this case some material adhered to the surfaces of the screw.

The delivery of the device fluctuates somewhat within each revolution, so that it appears some "smoothing" would be required in a final metering section of a disseminator using this principle. It has been noted that when the average discharge per revolution is plotted, a relatively smooth curve is obtained.

If a device of this type was required to provide a nearly constant delivery-versus time, speed programming would be required.

DECLASSIFIED IN FULL
Authority: EO 13526
Chief, Records & Declass Div, WHS
Date: MAY 17 2013

~~CONFIDENTIAL~~

~~CONFIDENTIAL~~

2.2 Experiment on Piston Feeding

To further explore the feasibility of using a simple piston as a feeding device in a BW disseminating store, a series of laboratory measurements on the forces in such systems have been initiated. During the reporting period one such experiment was made which determined the force required to translate a piston in a horizontal cylinder, thereby discharging the contained particulate material.

A description of the apparatus for this experiment appears in our last progress report.^{2.2.1} It consisted of a piston in the form of a thin Teflon disc, 38 mm in diameter and a lucite cylinder. The force was applied with a compression type spring scale which had been carefully calibrated. The apparatus was filled with Sierra Mistron No. 18 talc, the characteristics of which are given in Section 4.4 of this report. The atmospheric relative humidity during the experiment was 20 percent. The results presented in Figure 2.2.1 give the piston force and the mass of material delivered as a function of the linear displacement of the piston.

It can be seen from Figure 2.2.1 that the required force was constant over approximately one-half of the distance and then diminished, indicating reduced friction between the cylinder wall and the remaining particulate material. The magnitude of the maximum force was approximately 6×10^5 dynes, which corresponds to a very small pressure. Note that the length-to-diameter ratio of this device is approximately 4.7 which is comparable to a realistic maximum for a cylindrical section in an actual store.

2.2.1 General Mills, Inc. Report No. 2125, "Dissemination of Solid and Liquid BW Agents" (Unclassified Title) October 13, 1960, SECRET, pp. 42, 43

DECLASSIFIED IN FULL
Authority: EO 13526
Chief, Records & Declass Div, WHS
Date: MAY 17 2013

~~CONFIDENTIAL~~

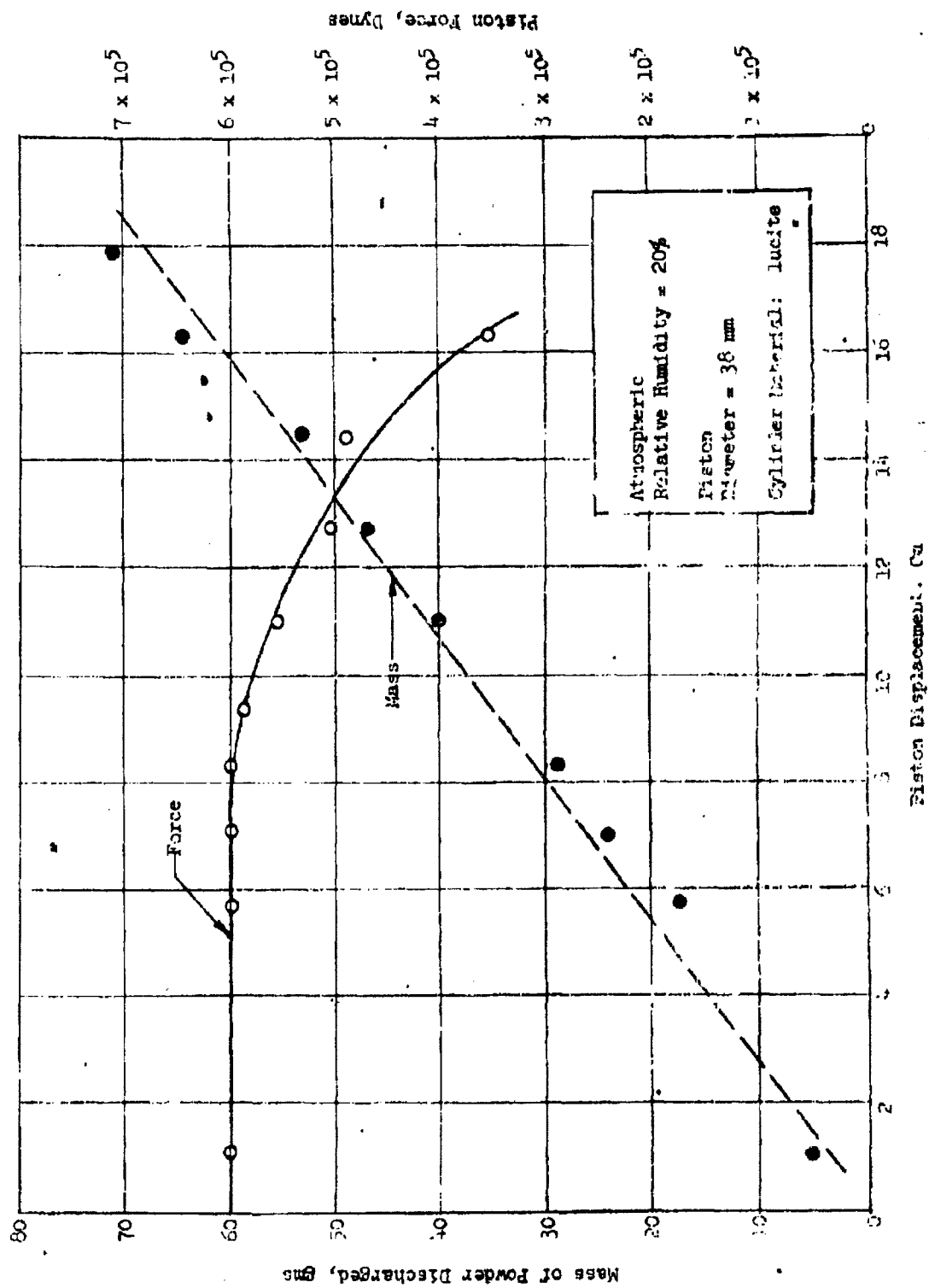


Figure 2.1 Characteristics of Piston Feeding Device,
Filled with Sierra Mistron No. 13 Talc.

The powder discharge rate per unit displacement remained essentially constant over the range studied, indicating that the compressive stress caused by the piston did not affect the bulk density in a non-uniform manner.

This simple experiment gave results which, by themselves, would attract one to this feeding system. However, variables such as scale factor and powder characteristics must be explored before adequate data are available.

DECLASSIFIED IN FULL
Authority: EO 13526
Chief, Records & Declass Div, WHS
Date: MAY 17 2013

- 16 -

~~CONFIDENTIAL~~

~~CONFIDENTIAL~~

3. DISSEMINATION AND DEAGGLOMERATION EXPERIMENTS

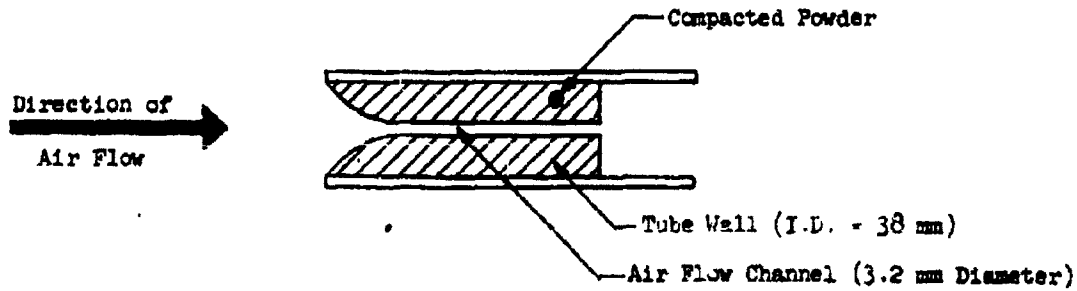
3.1 Investigations of Erosion as a Method of Dissemination of Finely Divided Materials.

It has been observed many times that a liquid or gas stream impinging on, or flowing over, the surface of a packed bed of finely divided material will carry with it some of the material which is removed by erosion. Since the delivery vehicles considered in this BW dissemination study will operate at velocities approaching sonic speed, the possibility of employing high velocity air streams to disseminate the solid BW agents by erosion deserves consideration.

A preliminary experimental evaluation of this technique has been made, in which the erosion rates were determined for models formed by compacting samples of finely ground flour and talc. The general conclusion from these experiments was that high velocity air streams will erode such materials at significantly high rates, but that the process is strongly dependent on the configuration and the packing procedure, as will be discussed in some detail in the following.

3.1.1 Initial Experiment

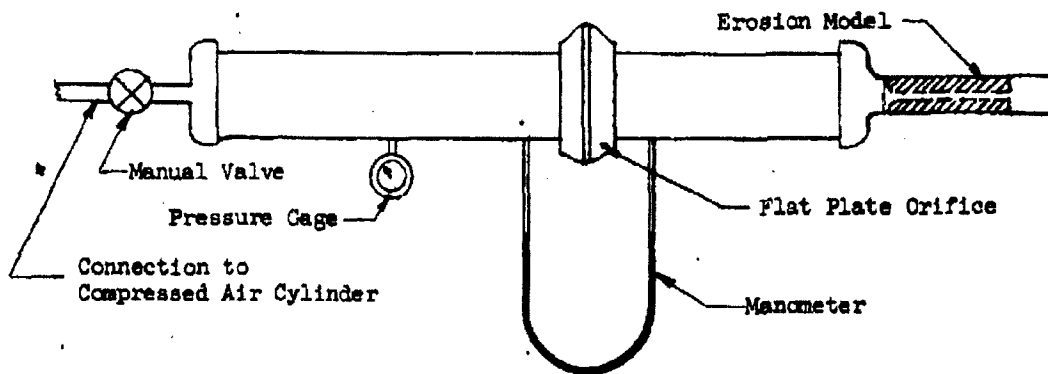
An initial erosion experiment was made with a model formed by compacting flour in a tube, with a metal insert in the center to form a channel for air flow. This model is sketched below.



~~CONFIDENTIAL~~

~~CONFIDENTIAL~~

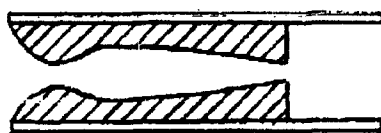
The model was attached to a system which permitted metering of the rate of air flow from the compressed air cylinder, through the erosion model, as sketched below.



The model was formed by compacting flour in the cylinder with a pressure of 1.5 atmospheres. The average mass flow rate of the flour was determined by weighing the model at time intervals of approximately 10 seconds. The air velocity through the system was maintained at sonic velocity throughout each erosion period.

The results of this initial experiment are shown in Figure 3.1.1. During the first 30 seconds the discharge of flour was intermittent. Then, continuous dissemination was observed. The appearance of the model after 105 seconds of exposure was as sketched below.

Direction of
Air Flow →
Air Flow



~~CONFIDENTIAL~~

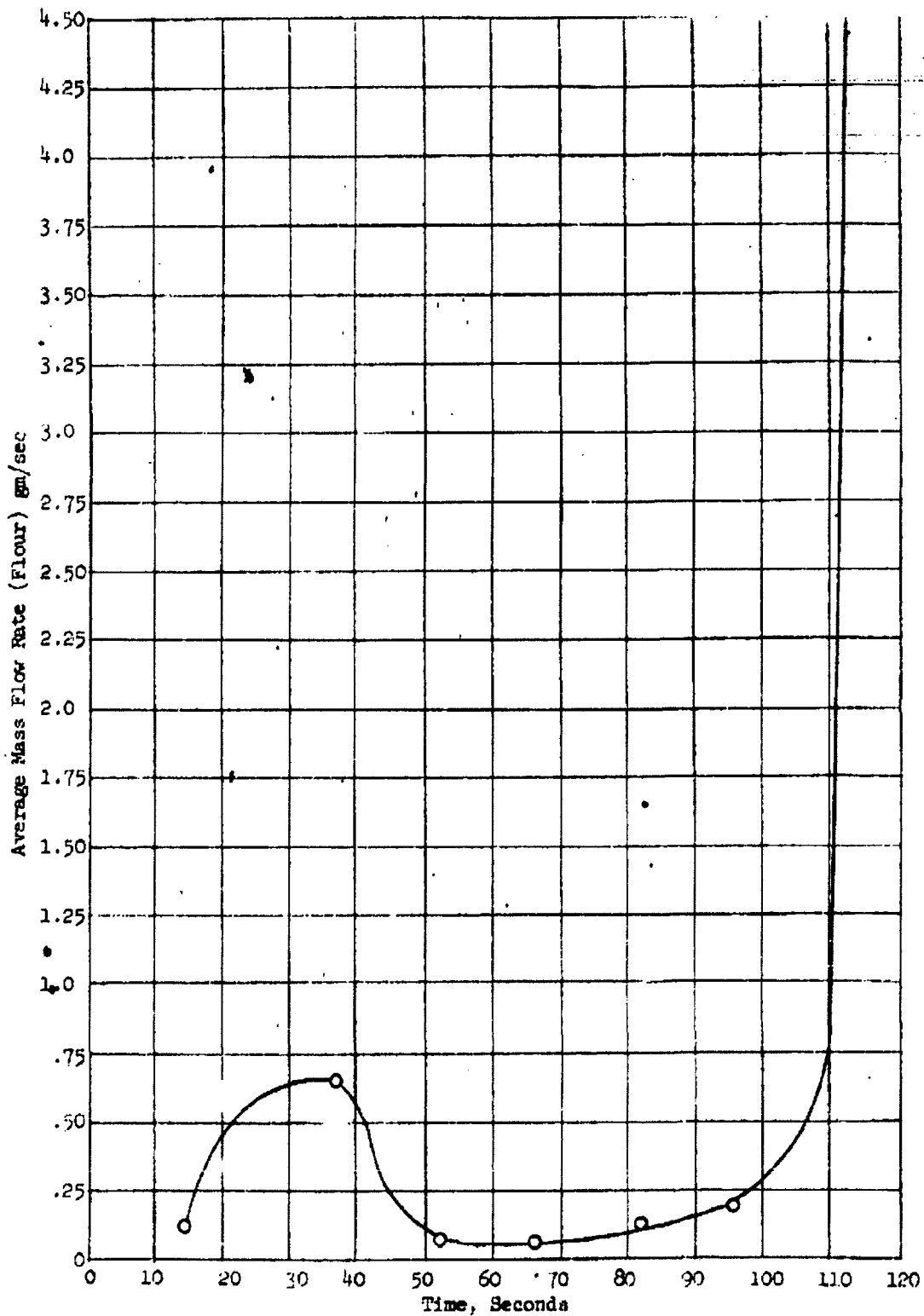


Figure 3.1.1 - Graph of initial flow test with Flour

~~CONFIDENTIAL~~

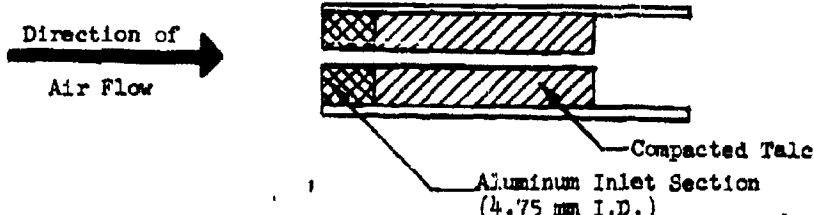
During the next 10 seconds, the form of the inlet was broken down and the mass flow rate of air increased sharply. This increased air flow caused very high erosion, and after 115 seconds the model was as illustrated below.



In an attempt to eliminate this sudden increase in flow caused by the inlet breaking down, the subsequent experiments, which were conducted with Sierra Mistron No. 18 talc, were conducted using a steel inlet section in the model, as discussed in Section 3.1.2.

3.1.2 Erosion Experiments With Talc

The model of revised design is illustrated below:



Two experiments were made with this configuration. The talc was compacted under a pressure of 1.5 atmospheres. The air pressure upstream of the model was maintained constant at 1.4 atmospheres absolute, with a mass flow rate (air) of 6 gm/sec.

Figure 3.1.2 shows typical photographs of the aerosol streams produced in these experiments.

DECLASSIFIED IN FULL
Authority: EO 13526
Chief, Records & Declass Div, WHS
Date: MAY 17 2013

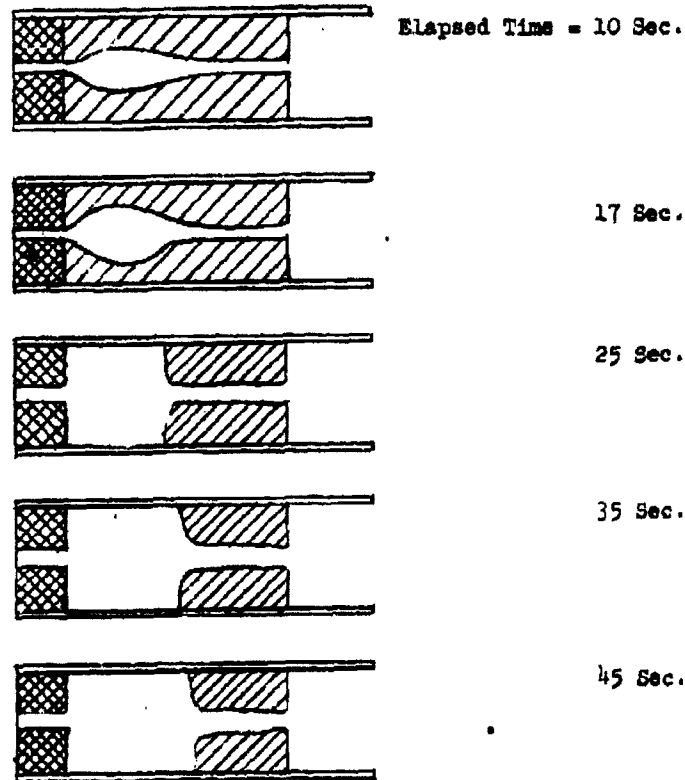
~~CONFIDENTIAL~~



Page determined to be Unclassified
Reviewed Chief, RDD, WHS
IAW EO 13526, Section 3.5
Date: **MAY 17 2013**

~~CONFIDENTIAL~~

The results for the first experiment with talc are given in Figure 3.1.3. It can be seen that the aerosol was discharged continuously, but with considerable variation in mass flow rate. The appearance of this model, as a function of time is illustrated in the sketches below.



The peak in Figure 3.1.3 at about 22 seconds is believed to be associated with the fact that the cavity reached the wall and the entire front section was discharged in a short period.

DECLASSIFIED IN FULL
Authority: EO 13526
Chief, Records & Declass Div, WHS
Date: MAY 17 2013

~~CONFIDENTIAL~~

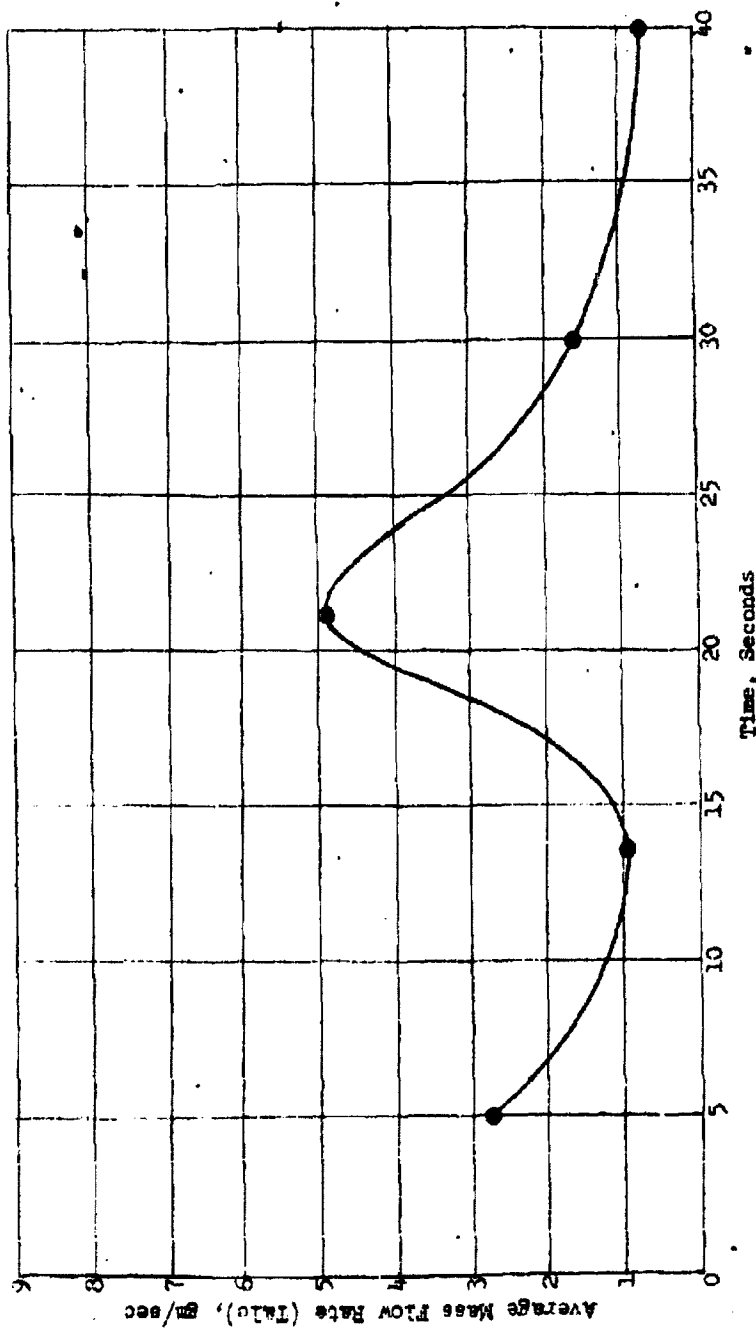
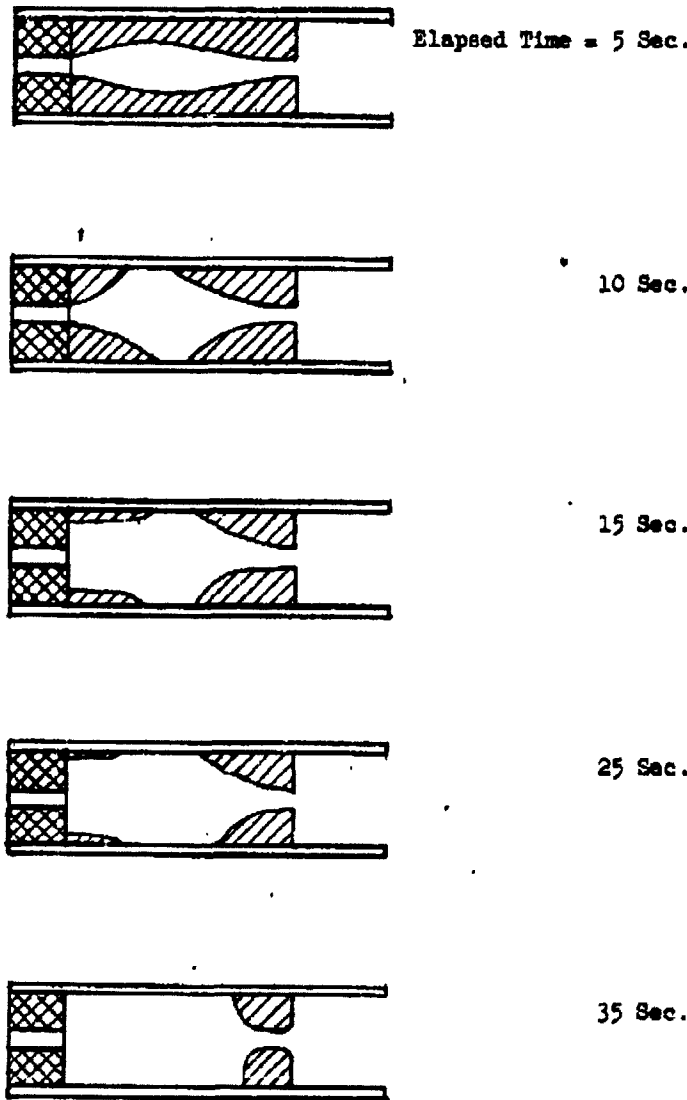


Figure 3.1.3 Average Mass Flow Rate Versus Time
for Erosion Type Aerosol Generator (Model 2)

~~CONFIDENTIAL~~

The results of the second experiment with talc are given in Figure 3.1.4. All measured conditions for this last were equal to those of the first experiment. (Figure 3.1.3) The appearance of the model as a function of time is illustrated in the sketches below.



~~CONFIDENTIAL~~

DECLASSIFIED IN FULL
Authority: EO 13526
Chief, Records & Declass Div, WHS
Date:

MAY 17 2013

~~CONFIDENTIAL~~

In this case, the rise in erosion rate near the 25 second mark was not as pronounced as in the first case. The variation between Figure 3.1.3 and 3.1.4 illustrates the fact that, with the techniques employed, this process is not a closely controllable one.

It is interesting to note that the most pronounced variations in powder flow rate occur while the volume just downstream of the inlet orifice is being cleaned out. After the cylindrical cavity is formed and the primary effect of further erosion is to increase the length of this cavity, the process is much more predictable.

Although these erosion experiments were quite rudimentary, they indicate that the erosion process is quite sensitive to geometrical configuration. It appears that a dissemination system of this type would be restricted to specific preparation procedures, and probably does not offer the flexibility desired in the solid agent dissemination system under study.

DECLASSIFIED IN FULL
Authority: EO 13526
Chief, Records & Declass Div, WHS
Date: MAY 17 2013

~~CONFIDENTIAL~~

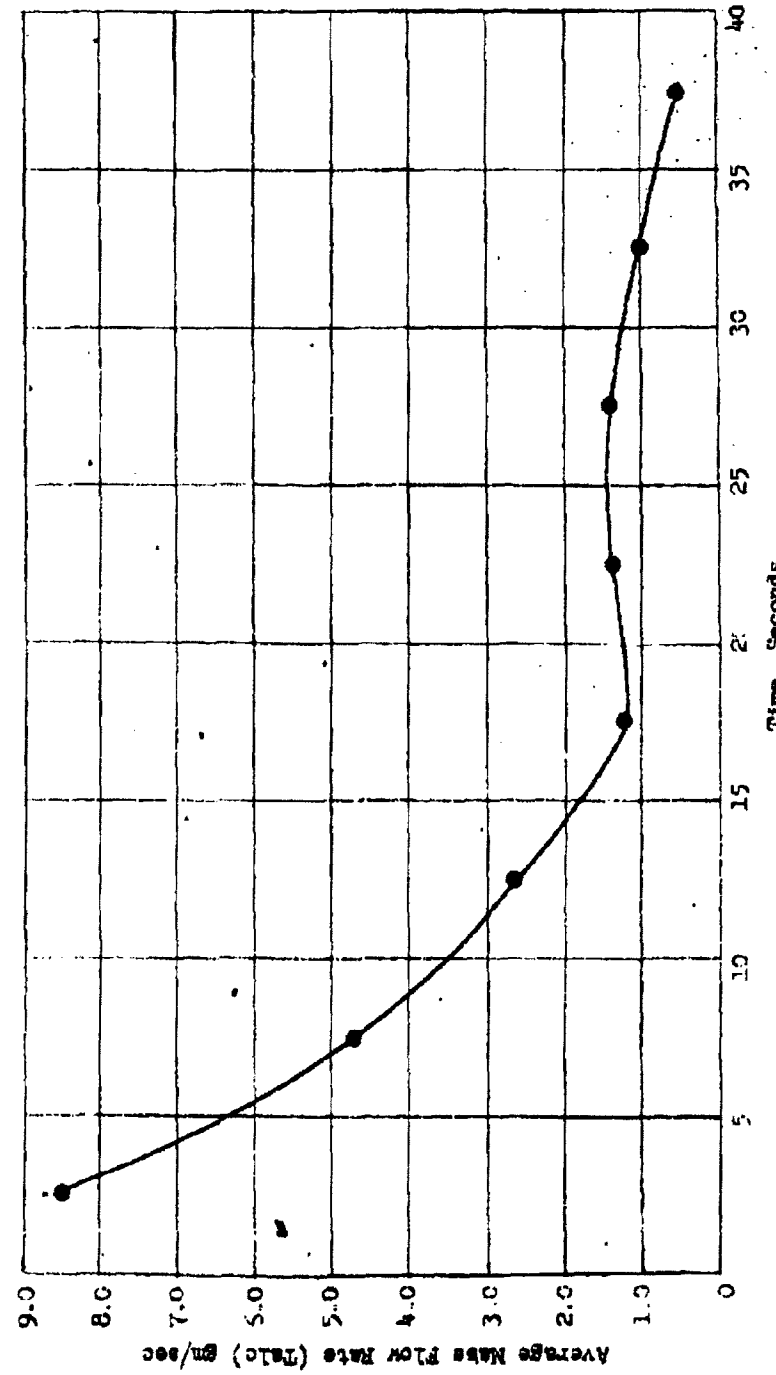


Figure 3.1.4 Average Mass Flow Rate Versus Time
for Erosion Type Aerosol Generator (Model No. 3)

~~CONFIDENTIAL~~

3.2 Experiments on the Use of Carbon Dioxide to Disperse Finely Divided Solids

Preliminary experiments have been conducted to explore the possibility of using liquid carbon dioxide as a carrier for solid BW agents. Carbon dioxide is generally considered to be compatible with viable agents (in the absence of water) and could also supply the energy required for feeding the material.

In these experiments samples of finely ground flour (7-9 microns MMD) were placed in carbon dioxide cylinders before adding the liquid. The objective was to explore the range of solids concentration which could be satisfactorily discharged from the cylinder.

The cylinders used in this work had a nominal liquid capacity of 5 pounds, and were fitted with an internal standpipe so that the liquid is discharged by the vapor pressure of the gas in the top of the cylinder.

A range of solids concentrations from 1/20 to 1/2 (solids/liquid mass) were explored. It was found that the highest concentration for which essentially all of the flour was removed (when the tank was discharged) was 1 part solids in 4 parts liquid by weight.

Microscopic inspection of samples collected on slides by impaction indicated that this process also deagglomerated the material quite well. The additional deagglomerating forces available in the slipstream of a high speed delivery vehicle would also be available to improve this process.

The potential advantage of a system of this type are (1) no external power is required for feeding the material, (2) the carbon dioxide may assist in the deagglomeration process, and (3) the system appears to be simple.

~~CONFIDENTIAL~~

~~CONFIDENTIAL~~

However, there are some very large weight penalties associated with the presence of the large quantity of inert liquid and the requirement for a pressure vessel capable of withstanding the vapor pressure of 60 or 70 atmospheres.

Further work on this concept has not been conducted due to these problems.

DECLASSIFIED IN FULL
Authority: EO 13526
Chief, Records & Declass Div, WHS
Date:

MAY 17 2013

~~CONFIDENTIAL~~

3.3 High Velocity Sampling Probe Tests

In connection with the experiments on deagglomeration by slipstream energy, a high velocity aerosol sampling probe has been designed and fabricated, as previously reported.^{3.3.1} This probe is designed to provide isokinetic sampling in the test section of the high subsonic blow-down wind tunnel and to decelerate the aerosol to a low velocity compatible with conventional sampling techniques such as membrane filters, impactors and impingers.

Before using this probe in the deagglomeration experiments, it was desirable to study its aerodynamic characteristics. Therefore, performance tests were conducted in a 22 x 22 inch subsonic wind tunnel, located at the Fluidyne Engineering Corporation, Minneapolis.

Four static pressure taps (open to the inside of the probe) were installed along the length of the probe at the following distances from the inlet:

No. 1 - 1 inch

No. 2 - 4 inches

No. 3 - 10 inches

No. 4 - 18 inches

These pressure measurements together with the wind tunnel stagnation and static pressure measurements provided the necessary data for calculations of the recovery pressure ratio and the diffuser efficiency.

^{3.3.1} General Mills Report No. 2125, "Dissemination of Solid and Liquid BW Agents" (Unclassified Title) October 13, 1960, SECRET, p. 27.

By using a vane-type vacuum pump downstream from the probe, the mass flow rates were controlled above and below isokinetic inlet conditions at free stream Mach numbers 0.5, 0.6, 0.7, and 0.8. The pump flow rate was calibrated against the inlet stagnation pressure in such a way that a pre-determined mass flow rate was obtained by setting a throttling valve upstream from the pump.

For the present application, it is intended that the probe will be mounted with zero angle of attack. However, to get a more complete understanding of its characteristics, it was felt necessary that an investigation of the effect of variable angle of attack be made at one Mach number. An angle of 5° at Mach number 0.5 was chosen for this purpose.

Figure 3.3.1 shows the diffuser pressure ratio, p/p_{0g} , plotted against the mass flow rate ratio w/w^* defined as follows:

p = static pressure at the different locations in the diffuser

p_{0g} = stagnation pressure of the tunnel free stream

w = mass flow rate in the diffuser

w^* = maximum mass flow rate in diffuser (i.e., choked throat condition - 0.945 lb/min)

Since the data at Station 3 were nearly identical with those at Station 4, they were omitted.

Due to a choked flow condition at $w/w^* = 1$, the curves drop sharply at this point.

At Station 4, the velocity is on the order of 10 feet/sec and the static and stagnation pressures are essentially identical. Thus, the curve through these data points represents the stagnation pressure recovery and

Page determined to be Unclassified

Reviewed Chief, RDD, WHS

IAW EO 13526, Section 3.5

Date: MAY 17 2013

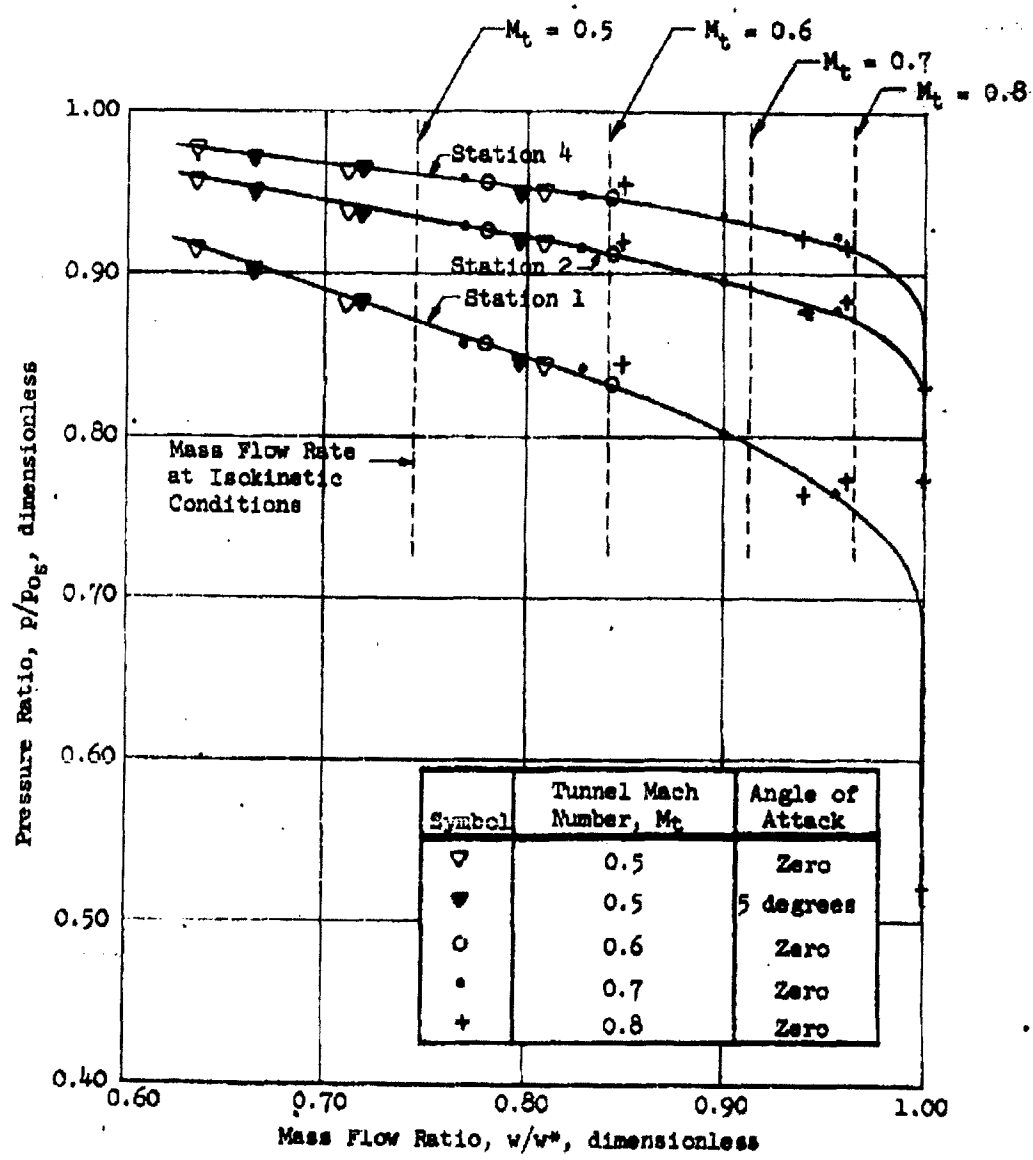


Figure 3.3.1 Pressure Ratio Versus Mass Flow Ratio
for High Velocity Sampling Probe

provides a good indication of the pressure losses due to separation and skin friction. The curve shows that the recovery pressure data are in good agreement for constant mass flow rates, with the exception of the data at Mach numbers 0.5 and 0.8 with angles of attack of 5° and 0° respectively. This seems to indicate that there was no severe separation at the inlet for these runs even though the flow rates were above and below the isokinetic inlet conditions. The very slight downward deviation of those values mentioned may be caused by inlet losses. However, they are small and it is believed that they will not be detrimental to the sampler operation. Since the pressure losses are the same for various stream Mach numbers at constant mass flow rates, it is felt that the loss is primarily due to skin friction.

The diffuser isentropic efficiency is shown as a function of the mass flow rate parameter in Figure 3.3.2. The term is commonly used and is defined as follows:

$$\eta_d = \frac{(h_4 - h_t)_i}{h_4 - h_t}$$

where h = static enthalpy

subscripts:

i = isentropic case

4 = diffuser station number

t = tunnel stream

It is possible to rewrite the equation in a more usable form by using well known thermodynamic relationships between energy, temperature and pressure.

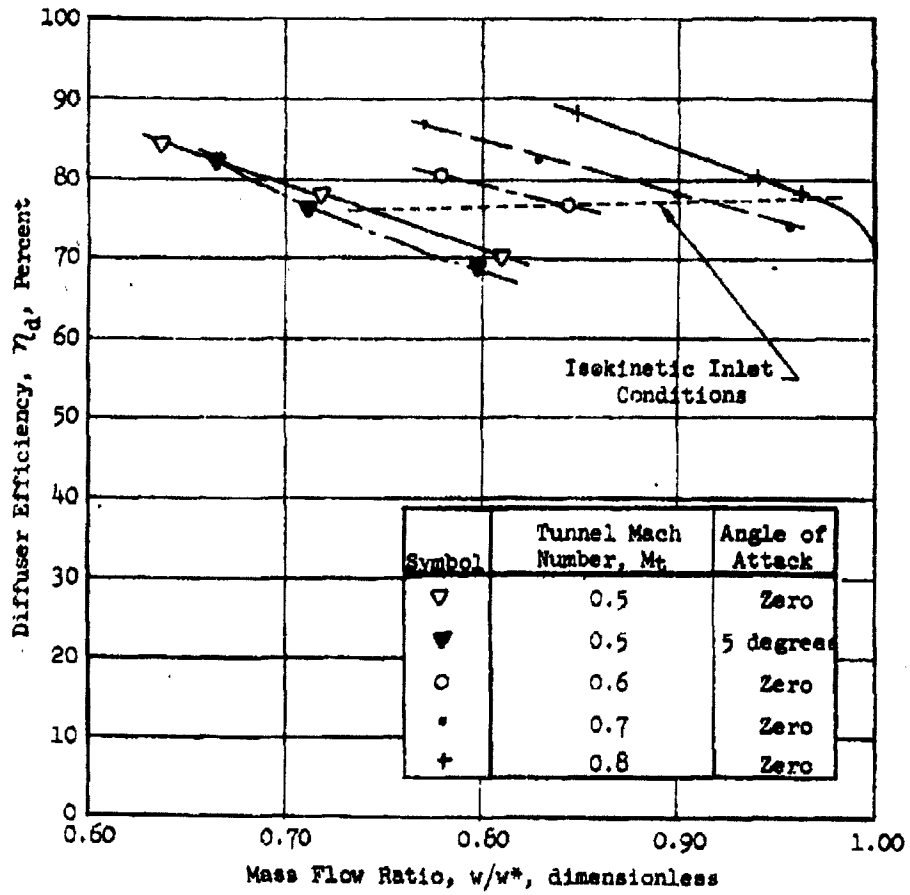


Figure 3.3.2 Diffuser Efficiency Versus Mass Flow Ratio
for High Velocity Sampling Probe

Page determined to be Unclassified
Reviewed,Chief, RDD, WHS
IAW EO 13526, Section 3.5
Date:

Thus,

$$\eta_d = \frac{(p_4/p_t)^{(\gamma-1)/\gamma} - 1}{\frac{\gamma-1}{2} M_t^2}$$

where p = static pressure

γ = ratio of specific heat values

M_t = tunnel Mach number

At isokinetic inlet conditions for all the free stream Mach numbers tested, the efficiency is nearly the same, approximately 77 percent. According to A. H. Shapiro^{3.3.2} efficiencies of 75 percent are most common in wind tunnel diffuser applications which are comparable to the sampling probe.

The tests at Mach number 0.5 at 5° angle of attack produced interesting results. At $w/w^* = 0.664$, substantially below the isokinetic condition, the efficiency apparently is not affected by the angle of attack. However, a rather sharp decrease appears to take place at a somewhat higher mass flow rate, indicating the slight effects of undesirable inlet conditions.

From Figures 3.3.1 and 3.3.2, it appears that the diffuser can be operated satisfactorily at stream Mach numbers up to 0.85. Also, an accurately calibrated vacuum pump is necessary for successful sampling.

3.3.2 Shapiro, A. H. *The Dynamics and Thermodynamics of Compressible Fluid Flow*, the Ronald Press Co., New York, 1: 152, (1953).

3.4 Deagglomeration Experiments

Preliminary deagglomeration experiments have been made, utilizing the high subsonic blow-down wind tunnel described in our previous technical report.

3.4.1

3.4.1 Apparatus

In these experiments a piston-type feeding device was used to discharge the sample of finely divided material into the test section of the wind tunnel. Figure 3.4.1 shows a cross-section of this device. The powder chamber is 0.80 cm in diameter and 2.5 cm in length, with a volume of 1.28 cm^3 . Operation of the release handle opens the slider valve and releases the compressed driving spring to permit discharge of the powder sample. The piston travels until its lower surface is flush with the inside surface of the wind tunnel wall. The actuating spring is interchangeable to permit variation of the discharge rate.

The feeding device is mounted on top of the wind tunnel, 12.4 cm downstream from the inlet nozzle, as shown in Figure 3.4.2.

3.4.2 Preliminary Experiments

The preliminary experiments discussed herein were performed before the high velocity sampling probe discussed in Section 3.3 was ready for use. The aerosol cloud from the wind tunnel was discharged directly into the laboratory. Glass microscope slides were mounted on a panel perpendicular to the high velocity jet, 2.4 meters downstream of the tunnel exit. Samples were collected on these microscope slides by impaction. This procedure creates a bias toward the larger particles, due to the tendency for

3.4.1 General Mills Report No. 2125, "Dissemination of Solid and Liquid BW Agents" (Unclassified Title) October 13, 1960, SECRET, p. 21.

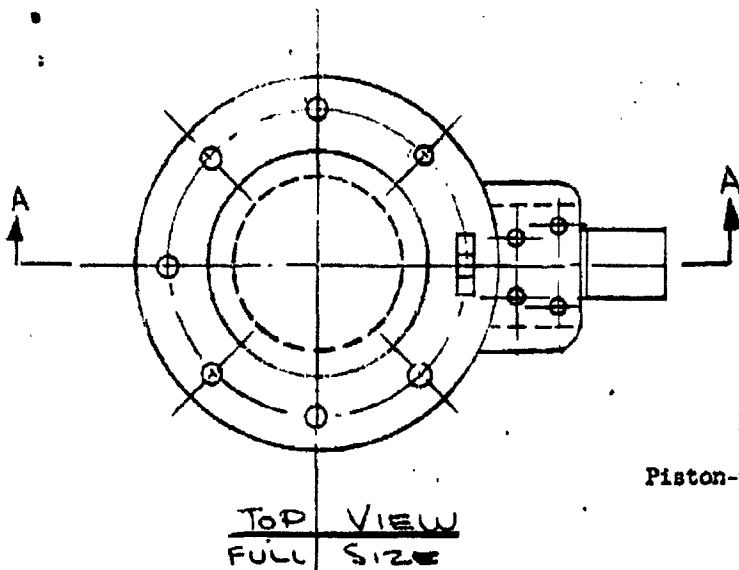
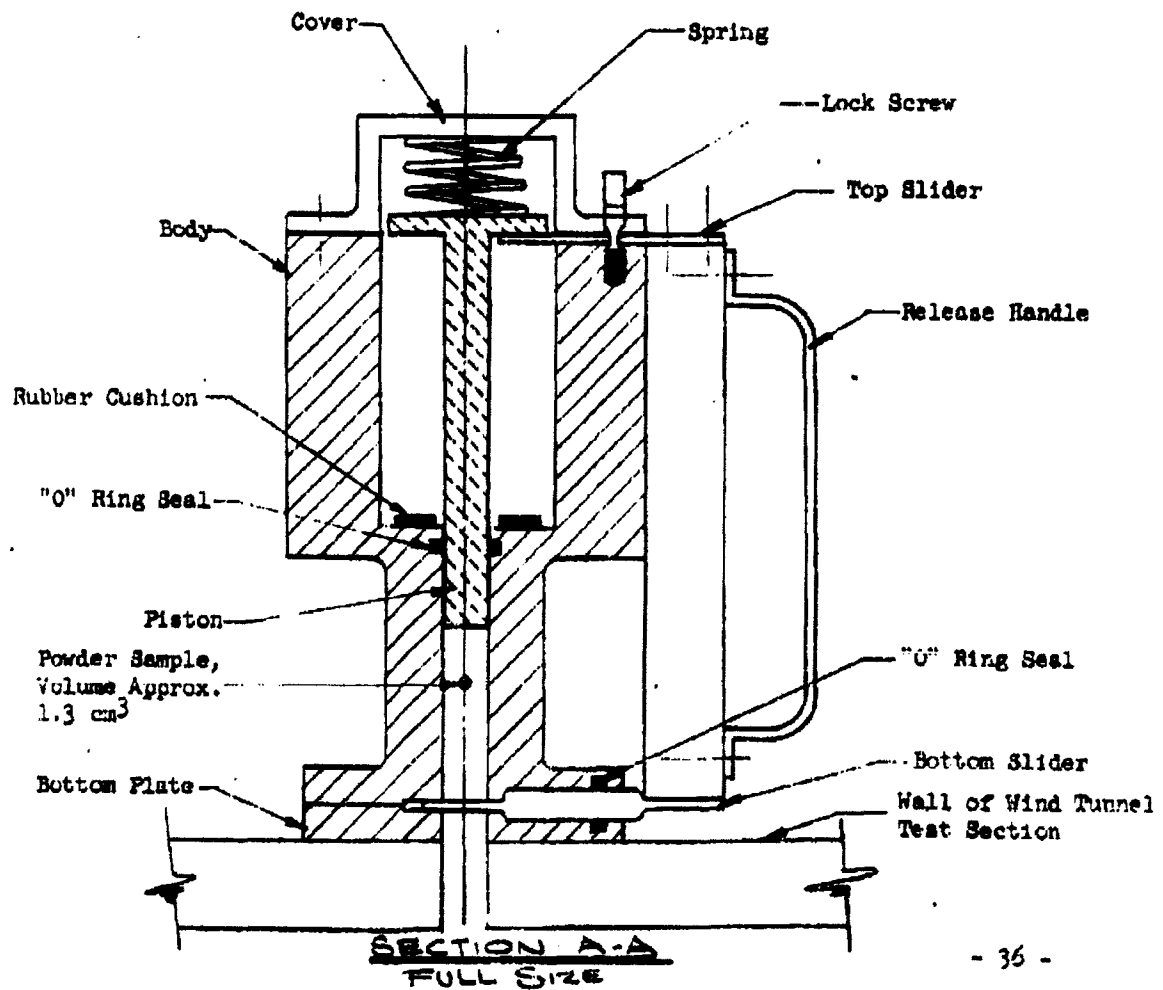
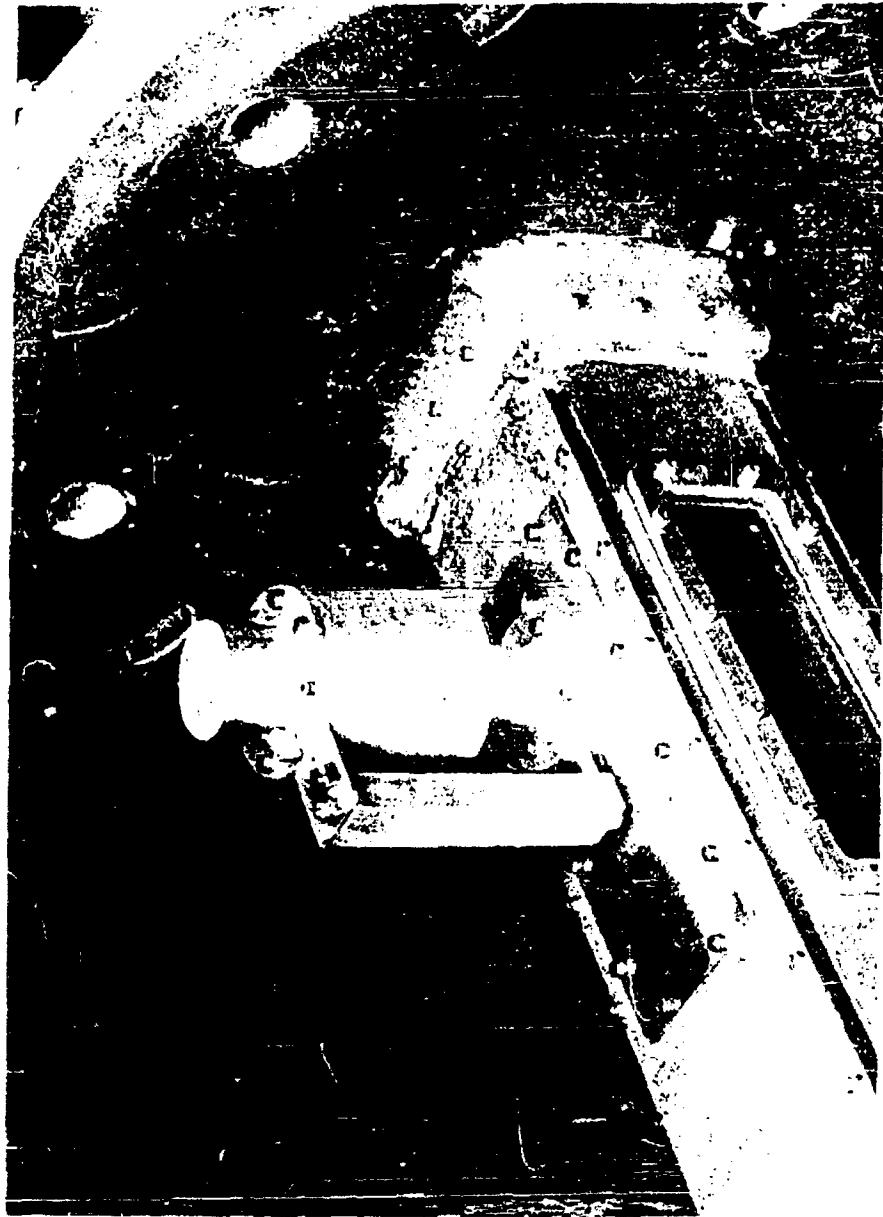


Figure 3.4.1

Piston-Type Feeding Device



- 36 -



Page determined to be Unclassified
Reviewed Chief, RDD, WHS
IAW EO 13526, Section 3.5
Date: MAY 17 2013

the smaller particles to follow the streamlines. Therefore, the experiments gave only an indication of the size of the larger agglomerates which were present in the aerosol stream.

Samples of talc and finely ground flour were disseminated in these experiments. The tunnel Mach number was 0.60 for the talc and 0.60 and 0.80 for the flour.

The mechanical operation of the disseminating device was found to be satisfactory. After releasing the piston, the powder appeared in the jet, downstream from the tunnel as a confined cloud.

Two methods were employed to obtain estimates of the agglomeration of the powders before the wind tunnel experiments. These were (1) microscope observation of a sample of the bulk material and (2) analysis of the particle size distribution by the Whitby centrifuge technique as described in Section 4.4. Figure 3.4.3 is a microphotograph (600X) of the flour before dissemination, showing large agglomerates. The talc, which is translucent and therefore difficult to photograph, did not appear to be agglomerated. However, the centrifuge results tabulated below indicate that both powders were not significantly agglomerated after being prepared for size analysis and centrifuged, since they were in the size range specified by the source of supply. An explanation for the difference between the flour photograph and the centrifuge results may be that the primary particles are held together weakly by moisture, and are broken apart in the process of dispersion for centrifuge analysis.

Page determined to be Unclassified
Reviewed Chief, RDD, WHS
IAW EO 13526, Section 3.5
Date: MAY 17 2013



Page determined to be Unclassified
Reviewed Chief, RDD, WHS
IAW EO 13526, Section 3.5
Date:
MAY 17 2019

<u>Material</u>	<u>MMD</u>	<u>GSD</u>	<u>Size Range</u>
Talc	2.3 microns	1.84	90% from 1 to 15 microns
Flour	6.55 microns	1.67	70% from 5 to 20 microns

Figure 3.4.4 is a microphotograph of the flour after dissemination. Many of the particles are in the 3-to-5 micron range and agglomerates are also present which are approximately 10 to 15 microns in size. Since the microscope field of view is quite limited, the photographs do not reveal the fact that there were also a few very large agglomerates approximately 500 microns in size. These large agglomerates were present to a much smaller degree in the aerosols produced when the Mach number was 0.80 than in the cases where the Mach number was 0.60.

These results, which are very preliminary, indicate that this dissemination device does not cause strong agglomerations during the ejection of these powders which cannot, in most cases, be broken up by the high subsonic air stream.

One important aspect of dissemination which can be studied with this model is diffusion of powders in a high velocity jet. It is believed that to efficiently deagglomerate powders it is necessary to accelerate them at a high rate in the air stream and to eliminate areas of very high concentration. Since there is a low velocity boundary layer along the tunnel wall, it is desirable to get the powder into the center of the stream where maximum acceleration can be achieved. Also, under such a condition there will be a minimum amount of powder collecting on the tunnel walls which may agglomerate and leave the tunnel in relatively large pieces.

Observations of the wind tunnel after these preliminary runs indicated that the main aerosol jet followed the upper tunnel wall. In the case of the talc tests there was only a small amount which adhered to the wall. On the contrary, in each of the flour runs a considerable amount of the material was collected on the wall extending back to the tunnel exit. It is believed that this aerosol flow condition was the result of a relatively low injection velocity. The necessity of sampling at different positions across the wind tunnel with the high velocity sampling probe in future tests is borne out by these tests.

In the use of an injection type model such as described here, two factors determine the penetration of the powder into the air stream: the injection velocity and the turbulent diffusion of the stream. Both of these parameters will be investigated in the subsequent studies.

Future studies will be carried out with talc, flour, and SM to determine the effects of the following factors:

- (1) air stream Mach number
- (2) injection velocity
- (3) agglomeration and powder compaction
- (4) air stream turbulence

The aerosol will be sampled by using the high velocity sampling probe and 76 mm dia., type AA, Millipore filters which have an 0.8 micron pore size. The particle distribution will be determined before and after each run by the microscopic and Whitby Centrifuge analyses.

Page determined to be Unclassified
Reviewed Chief, RDD, WHS
IAW EO 13526, Section 3.5
Date: MAY 17 2013

4. INVESTIGATIONS OF THE CHARACTERISTICS OF FINELY DIVIDED MATERIALS

4.1 Literature Search

As a result of the literature search on the properties of finely divided materials, several papers have been reviewed which contribute to the total understanding of the factors influencing behavior of bulk powders. These papers deal primarily with specific surface area measurements and the relation of size distribution to plasticity, dilatancy and force transmission in bulk powder.

4.1.1 Specific Surface Area

The specific surface area differs widely for powders of various chemical and physical types. Gas adsorption, air-permeability and microscopy methods have been used to determine values of the specific surface area of samples. For particles below 6 microns in diameter, the air-permeability method gives lower values than does microscopy or gas adsorption. The agreement between each method depends upon the size and other characteristics of the powder; also, the results from each method depend on a different characteristic of the powder.

D. H. Mathews^{4.1.1} compared the specific surface areas of nineteen fine powders by: (a) adsorption of nitrogen at 77°K and (b) air-permeability method described by Rigden^{4.1.2}. By method (a), the specific area measured was larger. Mathews suggested that the discrepancy between the two methods of measurement may be due in part to the existence of an internal surface in some powders which were not measured by the air-permeability method.

4.1.1 Mathews, D. H. Journal Appl. Chem. 7, Nov. 1957

4.1.2 Rigden, P. J. Journal Soc. Chem. Ind. 66: 130, 1947

Page determined to be Unclassified
Reviewed Chief, RDD, WHS
IAW EO 13526, Section 3.5
Date:

Cartwright, Wheatley and Sing^{4.1.3} determined the specific surface area of different samples of silica and glass spheres in the size ranges 1-12 microns by: (a) gas-adsorption, (b) air-permeability and (c) microscopy. They established an empirical relationship between the diameter calculated from microscopic measurements of volume and the diameter calculated from the specific surface by gas-adsorption. The relationship was shown to apply to all samples tested except unetched quartz.

A study of how the surface area depends on the conditions of drying and storing of precipitated alumina was made by Harris and Sing.^{4.1.4} Considerable variation in surface area was found. This study of the literature reveals the importance of surface area as a characteristic of powder; and measurements by the various methods indicate the existence of a large internal surface area in many powders.

4.1.2 Relation of Size Distribution to Plasticity, Dilatancy and Force Transmission in Bulk Powder.

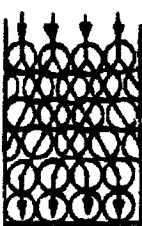
Carl Ludwig^{4.1.5} stated that the most important property of loose bulks, insofar as agglomeration is concerned, are particle size distribution and plasticity. He noted that uniform size particles are not the optimum for agglomeration. Clusters of uniform size particles are easily separated along symmetrical planes and resist movement along non-symmetrical packings of random assembly.

4.1.3 Cartwright, J., K. Wheatley, and K. S. W. Sing. J. Appl. Chem. 8, April 1958

4.1.4 Harris, M. R., K. S. W. Sing. J. Appl. Chem. 7: 397, 1957

4.1.5 Ludwig, Carl. Chem. Eng., 156, Jan. 1954

Ludwig illustrated how a cluster having a predominance of one size forms a truss-like structure in compression and resists compressive flow. Conversely, a random assembly of particles varying in size is plastic and can be molded or compressed.



Uniform Particle
Size Distribution



Random Particle Size,
Non-Symmetrical Pack

Brown and Hawksley^{4.1.6} studied the mechanism of the flow of particles in two-dimensional beds. Their study of the literature revealed that dilatancy is an important factor in the flow of granular materials. A dilatant material is one which increases in volume when the shape is changed, due to wider spacing of the particles. Dilatancy was found to apply to any stable regular or irregular packing of graded or ungraded particles of any size. Photographs of their two-dimensional model consisting of a single layer of ball bearings were scrutinized and conclusions drawn. One important conclusion was that inhomogeneity in a bed under deformation is caused by movement of groups of particles. Dilatancy may be unnoticeable in loose packings, since large reductions in volume may result from collapse of the particle structure.

4.1.6 Brown, R. L., and P. G. W. Hawksley, "Fuel in Science and Practice,"
26: 159-73, 1947

W. Mead^{4.1.7} describes several of Osborne Reynold's experiments which illustrate dilatancy. One example is described as follows: a rubber balloon is filled with sand, shaken, and enough water is added to just fill the voids. When the balloon is deformed, dilatancy increases the void volume so that more water is required to fill all the voids.

Jenkin^{4.1.8} tried repeatedly to measure the "coefficient of friction" of granular material to confirm theories on earth pressure. His failure to obtain reproducible results led to a study of the influence of dilatancy on force transmission in packed beds. Although this work was not comprehensive, it provides a background for further study of the problem.

An analysis of force transmission has been made on the current project which is presented in Section 4.2 which follows.

4.1.7 Mead, W. J., Journal of Geology 33: 685, 1925

4.1.8 C. F. Jenkin, "Pressure Exerted by a Granular Material: An Application of the Principle of Dilatancy" Proc. Roy. Soc., A, 1931.

4.2 Theoretical Investigations

An analysis has been made of static load transmission in particulate packings which reveals several possibilities for future research on the properties of finely divided materials. This analysis is presented below.

No general theory of load transmission or stress distribution in granular packings is available at the present time. Consequently, an effort is being made to develop a theoretical basis for studying the stress-yield characteristics of particle beds. These characteristics are expected to have an important bearing on the handling properties and characterization tests for various dry agent materials.

In examining the characteristics of particulate packings, it appears that a distinction must be drawn between solid, essentially elastic particles such as sand, glass beads, metal shot, etc., and porous compressible materials such as biological materials, flour, cornstarch, etc. In the former case, the concept of dilatation may hold the key to load transmission within the bed. A simple and interesting example of the role played by dilatancy is given below for a hexagonal packing. In general, random packings are found to be statically indeterminate so that some knowledge of the stress-strain or compressibility characteristics of the material is required in order to determine the load distribution in the bed. For beds composed of solid elastic elements (glass beads, shot, etc.) an analysis based on the elastic properties of aggregates of the particles should enable a specification of the stress distribution in the bed. Certain restrictions on the stress distribution must be observed, however, such as limits in permissible tensile stresses.

Page determined to be Unclassified
Reviewed Chief, RDD, WHS
IAW EO 13526, Section 3.5
Date: MAY 17 2013

It appears likely that an essentially different approach may be required for compressible materials since the yield stresses are probably related to the compaction of the material which occurs during loading. Materials of primary interest in the present study are expected to fall into this category. Investigations of both types of materials are being undertaken in order to gain as much insight as possible into the behavior of particle beds as it affects the handling and conveying aspects of dissemination systems for dry materials.

4.2.1 Analysis of Static Load Transmission in Granular Packings

Considerable work has been done in studying the properties of granular packings made up of solid particles. These packings are characterized by dilatant behavior. Thus if a packing has a volume V in an initial equilibrium state, the volume will generally increase by ΔV when a displacement is produced within the bed. If the bed volume is fixed, experiments indicate that motion of the granular material within the bed is impossible without fracture of the granules.^{4.2.1} With no confinement, pressures applied to the bed ultimately work against the weight of the material. The work done by the applied loading can be equated to the change in potential energy of the system plus the work done against friction in displacements of material in the bed. In general, the elastic energy stored in the bed must be included in the potential energy of the system, although in many instances this energy may be omitted with negligible error. The above

^{4.2.1} C. F. Jenkin, "Pressure Exerted by a Granular Material: An Application of the Principle of Dilatancy" Proc. Roy. Soc., A, 1931, 33, 53.

statement may be formulated in terms of the equation:

$$\delta'W = F \delta'x = \sum_1^n w_i \delta'y_{i,i} + \delta'W_f + \delta'P \quad (1)$$

where F is the applied force, $\delta'P$ is the change in elastic energy stored in the bed, and $\delta'W_f$ is the frictional work done in displacing the bed. The term $\sum_1^n w_i \delta'y_{i,i}$ is the change in potential energy of the bed summed over the n particles contained in the bed. Although the general energy relationship expressed by Equation (1) is not susceptible to straightforward analysis, it is frequently possible to justify omission of the elastic energy term $\delta'P$ in practical calculations. Furthermore, the frictional term $\delta'W_f$ may be approximately evaluated in some instances (an example is presented in the following section of this report). An important consideration in applications of Equation 1 is that complex static internal load distributions do not have to be determined in order to compute the work done on the bed since no net work is done by such forces. Of course, this is not true along lines of slip where frictional dissipation occurs. It will be noted that for packings composed of hypothetical frictionless, inelastic particles, Equation 1 reduces to:

$$F \delta'x = \sum_1^n w_i \delta'y_{i,i} \quad (2)$$

For granular materials, it appears that the relative displacements of particles in a bed may be related through the interparticle geometry of the bed. Thus if a force F is applied at a point in the packing, producing a small local displacement $\delta'x$, displacements $\delta'y_{n,i}$ will be developed in a

manner dependent essentially on the configuration of the particles in the bed. In general, these displacements would have to be determined on a statistical basis. However, for regular packings the displacements may be easily found in many cases, as illustrated in the following discussion.

4.2.2 Static load transmission in regular packings.

The basic principles presented in the above discussion find a ready application to regular packings of discs or spheres. Two-dimensional arrays are considered herein for the sake of simplicity. Extension of these results to three-dimensions does not appear to present any basic difficulty, but this will be deferred to a later report.

4.2.2.1 Square Arrays. The simplest regular packing is the square arrangement illustrated in Figure 4.2.1. For a bed of n tiers, the force per contact at the floor is nW where W is the weight of each element. It is clear that this force is not altered if one of the discs (or spheres) in the bottom row is displaced upward, since only those discs lying directly above the bottom disc are affected. This result is not altered by friction, assuming that no horizontal compression is applied to the bed. A second square arrangement is obtained by arraying the contacts between discs along lines inclined 45° to the horizontal as illustrated in Figure 4.2.2. Neglecting friction, it is again found that no increment of force is required to displace a disc at the bottom of the pile.

4.2.2.2 Hexagonal Arrays. The hexagonal arrangement of discs is much more interesting. Two regular configurations are possible as shown in Figures 4.2.3 and 4.2.4. Considering first the configuration shown in Figure 4.2.3,

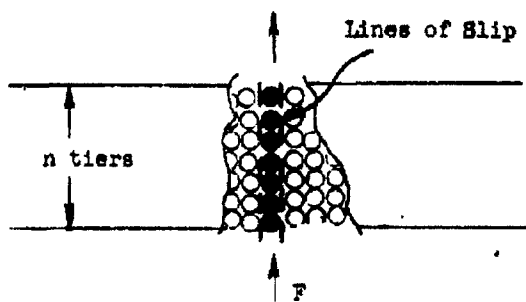


Figure 4.2.1. Vertical Square Array

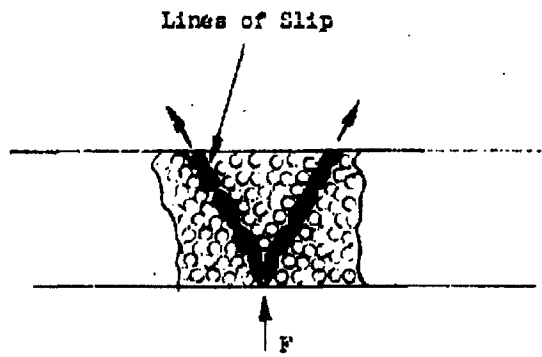


Figure 4.2.2. 45° Square Array

Page determined to be Unclassified
Reviewed Chief, RDD, WHS
IAW EO 13626, Section 3.5
Date:

MAY 17 2013

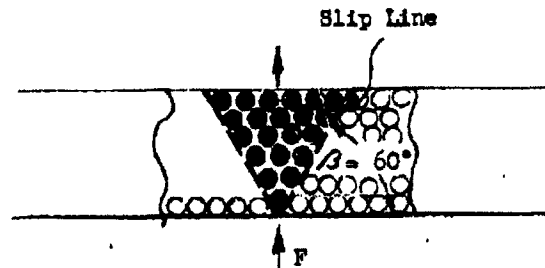


Figure 4.2.3. Hexagonal Array - Configuration I

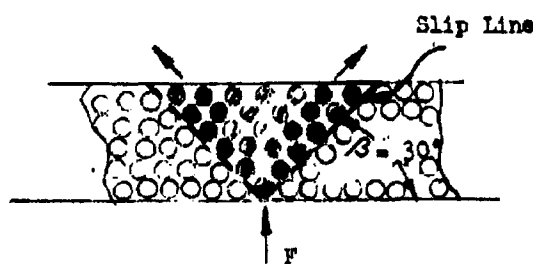


Figure 4.2.4. Hexagonal Array - Configuration II

it is found that the upward displacement of a disc at the bottom of the pile will raise all of the discs in the triangular region MNO. Along the slip lines MO and NO, the diagonal contacts marked with a small circle are opened while additional loads are transferred to the horizontal contacts. For frictionless discs the loading can be found very easily. It follows immediately from Equation 2 that the force F is simply the weight of the discs contained in the region MNO, i.e.:

$$F = \frac{n}{2} (n + 1) W \quad (3)$$

If m discs at the floor level are displaced the total force is:

$$F = n \left(m + \frac{n-1}{2} \right) W \quad (4)$$

The two end discs each support the load:

$$F' = \frac{n}{4} (n + 3) W \quad (5)$$

while the interior discs merely support the discs directly above them. This is a two-dimensional analog of the three-dimensional platform (Jolly balance) tests reported in our First Quarterly Progress Report.

The horizontal loads X_i applied to the discs lying on the diagonal OM are given by the formula:

$$X_i = \frac{iW}{\sqrt{3}} \quad (i = 1, 2, \dots, n) \quad (6)$$

where i denotes the i^{th} row of discs from the top of the bed. An approximate analysis of the effects of friction can be carried out by adding to

the load given by Equation 3 the frictional loading along the slip lines.

$$F = \left(1 + \frac{\mu}{\sqrt{3}}\right) \frac{n}{2} (n+1) W \quad (7)$$

where μ is the coefficient of friction. This result depends on the assumption that the contacts along OM and ON are simultaneously on the point of slipping.

Another hexagonal configuration is shown in Figure 4.2.4. Displacement of a disc at the point "O" by an amount δy clearly displaces the discs directly above "O" by an equal amount. However, the discs on either side of this vertical column are displaced at an angle as shown on the figure, the upward component of this displacement being $\frac{1}{2} \delta y$. Using the energy principle expressed by Equation 2 the yield force for this case is:

$$F = (n+1)(n-1)W, \quad (8)$$

corresponding to n tiers of discs. Comparing the above result with that obtained for the first hexagonal configuration on the basis of equal bed depth h , the following results are found (for large n):

Configuration I:

$$F = \frac{h}{\sqrt{3}d} \left(1 + \frac{2h}{\sqrt{3}d}\right) W \quad (3')$$

Configuration II:

$$F = \left(\frac{h}{d} + \frac{3}{2}\right) \left(\frac{h}{d} - \frac{1}{2}\right) W \quad (3')$$

These results are valid for large values of $\frac{h}{d}$. By inspection of these equations it can be seen that the yield force for the first configuration approaches two-thirds that of the second configuration for large h/d ratios.

The slip line in the above examples of regular packings corresponds to the so-called angle of internal friction, β .^{4.2.2} Generally, experimental values of β lie in the range 60° plus to 90° , whereas the theoretical values for regular packings correspond to 90° , 60° and 30° , according to the present analysis. For skewed regular packings and for random packings it is apparent that intermediate angles may be obtained. In random arrangements, local slip lines which vary from point to point may lead statistically to an overall angle of slip for an aggregate of granules, which may be interpreted as the internal angle of friction. Some investigations along this line are planned for the future. Other areas which will be studied include:

(1) Investigation of the load distribution in particulate beds on the assumption that the material behaves as a continuous medium. It is anticipated that analytical techniques from the theories of elasticity and plasticity might be brought to bear on the problem when viewed in this light. For compressible, compactible materials it appears likely that a theoretical approach along these lines would be very fruitful in conjunction with experiments to typify the compressibility and yield-stress characteristics of these materials - data which would be required for design. The ultimate goal of these studies is to relate the static behavior of particulate packings to basic physical properties of particulate materials.

(2) Flow properties of particulate materials will be studied insofar as possible for those materials capable of flow. No work of a general

4.2.2 Zenz and Othmer "Fluidization and Fluid-particle Systems" Reinhold Publishing Corp. New York (1960).

nature has been done to date along these lines aside from a survey of available literature.

In future work, an effort will be made to define conditions for the onset of flow (from a study of static yield characteristics as discussed above) and to examine the types of flow possible.

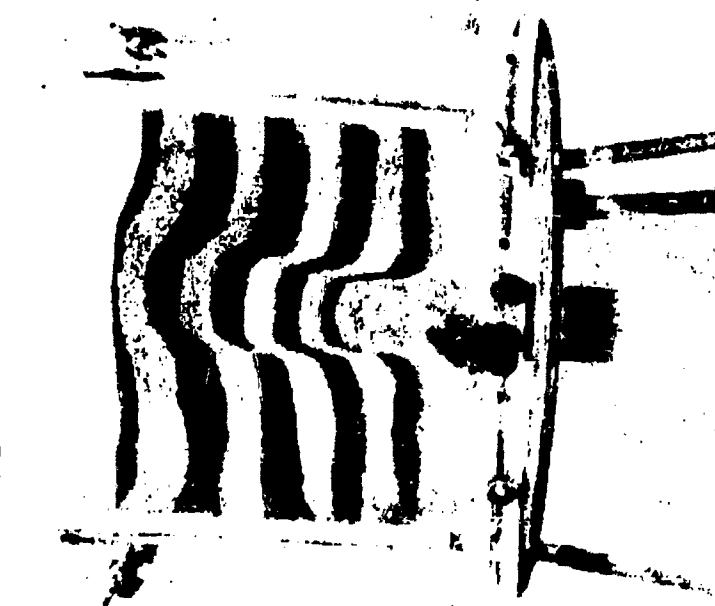
4.3 Experiments on Characteristics of Powders

Experiments of three types are discussed in this section. These deal with (1) translation of particles above a moving piston, (2) gravity flow of particles, and (3) the torque required to rotate a helical screw configuration in a powder bed. These experiments are discussed in the paragraphs which follow.

4.3.1 Translation of Particles Above a Moving Piston

An experiment was conducted to visually explore the translation of relatively large particles above a moving piston. The apparatus is shown in Figure 4.3.1. The material used in this experiment was steel shot, 200 to 300 microns in diameter. Alternate layers were colored so that the relative motion could be seen. As the piston was moved upward, the material above the piston was translated both vertically and horizontally. In Figure 4.3.1 note that the vertical displacement of the piston is many times larger than the vertical displacement of the top of the bed. Likewise, note that the width of the area which is disturbed on the surface is several times larger than the width of the piston.

It can also be seen that the boundaries of the displaced material are not closely defined, indicating the difficulty of applying theoretical analyses to a problem of this type. It appears that determination of the total volume displaced by the piston, may give a useful identifying characteristic of the material being studied.



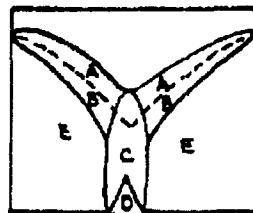
Page determined to be Unclassified
Reviewed Chief, RDD, WHS
IAW EO 13526, Section 3.5
Date: MAY 17 2013

4.3.2 Gravity Flow of Particles

The apparatus shown in Figure 4.3.1 and the particle coloring technique were also used to study gravity flow characteristics. The 200-300 micron steel shot was also used in this experiment.

After opening the discharge orifice, the upper part of the bed did not show movement until the material in the vicinity of the opening was discharged. Dilation was quite evident at this point.

The following sketch is useful in describing the subsequent flow.



Region A slides over Region B, and Region B slides over the stationary Region E. Region B moves more slowly than A. Region C consists of particles from both Regions A and B. Once the particles are near or in Region D, they fall at a much larger velocity. The angles the regions make with the horizontal remain constant during discharge. When the Regions A and B contact the orifice, the discharge quickly ends.

This experiment illustrates the fact that the gravity flow process is dependent on very localized conditions. In the process described above, the slope of the boundary between Regions B and E may be a useful identifying characteristic of the material.

4.3.3 Torque Required to Rotate a Helical Screw Configuration in a Powder Bed.

Measurements of the torque required to rotate a screw configuration in a powder bed have been made to explore the usefulness of this approach to identification of powders:

The apparatus used in these measurements is described in Section 2.1 of this report. It consists of a helical screw 44 mm in diameter, enclosed in a lucite cylinder with an interval diameter of 51 mm.

As a first step, the reproducibility of measurements of the torque required to rotate the screw was evaluated. In a series of 50 tests, the torque required to rotate the screw (when it was filled with Sierra Mistron #18 talc) was found to be 3.66×10^5 dyne-centimeters, ± 7 percent. (The particle size distribution of this material is given in Section 4.4 below.) This reproducibility indicates that the variations introduced by the filling process are relatively small.

The torque required to rotate the same configuration in a bed of poly vinyl alcohol powder was found to be approximately 50 percent of that required for the talc. This was a most interesting finding, since the bulk density of the p.v.a. is 0.569 gm/cm^3 while the density of the talc is 0.222 gm/cc . The data from the disc-lifting experiment previously described^{4.3.1} showed a strong density dependence. These torque measurements are apparently more sensitive to friction between particles.

We plan to extend these experiments to other materials and flow conditions.

4.3.1 General Mills, Inc. Report No. 2125, "Dissemination of Solid and Liquid BW Agents" (Unclassified Title) October 13, 1960, SECRET, p. 46.

4.4 Experimental Particle Size Analysis

In connection with the experimental work which has been and will be conducted in the fields of characterization, feeding, dissemination and deagglomeration of finely divided solid materials, the particle size distributions of several materials have been measured. The Whitby centrifuge technique was employed to determine the particle size distribution of bulk samples of three separate lots of SM, samples of Sierra Mistron No. 18 talc and also General Mills' "Jet" flour, which is a finely ground high protein flour.

The apparatus used in this work is the current model of the Whitby centrifuge equipment, manufactured by the Mine Safety Appliances Company. This apparatus includes a two-speed (600-1200 RPM) centrifuge, an 1800 RPM centrifuge and a centrifuge tube viewer, which is an optical device for measurement of the sediment height in a centrifuge tube.

4.4.1 Centrifuge Operating Principle

This particle size analyzer operates on the principle of sedimentation in a liquid. Whitby's original work^{4.4.1} fully describes the apparatus and method of application. The use of the centrifuge method greatly decreases the time required to analyze particles in the 1 to 5 micron size range. As an illustration, Whitby states that an analysis of A.C. Fine Test Dust (68.2% less than 12 micron diameter) that would take 54 hours by natural sedimentation can be accomplished in about 25 minutes by centrifugal analysis.

^{4.4.1} Whitby, K.T., ASHAE Journal Section, Heating, Piping and Air Conditioning, January 1955 (page 231) and June, 1955 (page 139-45).

Most centrifuge methods of size analysis start with an initially homogeneous suspension of particles in the tube. Serious problems exist in using this method since:

(1) particles of various sizes are settling out of suspension at any given time, and (2) the forces acting on the particles vary with the radius in the centrifuge. These factors make impossible an exact solution to the differential equations that describe the rate of sedimentation. These problems are overcome in the Whitby centrifuge by all of the particles being initially situated in a layer at the top of the sedimentation liquid.

The procedure used with the Whitby centrifuge is briefly summarized as follows: (1) the clean tube is filled to a line near the top with a suitable sedimentation liquid, and placed in the viewer; (2) a suspension of particles is made up (by blending) in a liquid that is miscible with the sedimentation liquid and has a slightly lower density and a slightly higher viscosity; (3) an aliquot of this suspension is placed in the feeding chamber and released in such a way as to leave a sharp layer of suspension on top of the sedimentation liquid; (4) then, at time intervals calculated from Stokes' law for the desired sizes, the height of the sediment in the capillary is read. Sedimentation is allowed to proceed under gravity for a predetermined period, then the tube is transferred to the lowest speed centrifuge and rotated for a precalculated time. The tube is removed to read the sediment height and then is replaced in the centrifuge for the next time interval. This is continued until there is no change in sediment height or until the last centrifuge time in the schedule has been run.

The procedure for calculation of the time schedules for the gravity settling period and the centrifuge operating periods is outlined in Appendix A of this report.

The direct results of this experimental size analysis are values of the percentage (by weight) of material of particle sizes smaller than each of several preselected particle diameters. These values are proportional to the ratio of the sediment height in the capillary of the centrifuge tube at the end of the time period (corresponding to the size in question) to the total sediment height at the end of the analysis. These data are conventionally plotted as the cumulative distribution on log normal graph paper. A straight line on this plot of percent-finer-than-size versus particle diameter, indicates a log normal size distribution. The mass median diameter (MMD) and the geometric standard deviation (GSD) may also be determined from a plot of this type.

4.4.2 Results

The results of these particle size determinations are presented in Figures 4.4.1 through 4.4.5. Each of these graphs gives data from two separate determinations so that the reproducibility of the data is illustrated.

With respect to the three separate lots of SM (Figures 4.4.1 through 4.4.3) it is interesting to note that sample GBL B-08070X which had been stored since its preparation several years ago had an average MMD of 4.9 microns, while the other SM samples (which were prepared in 1960) had average MMD values of 3.20 and 3.25 microns.

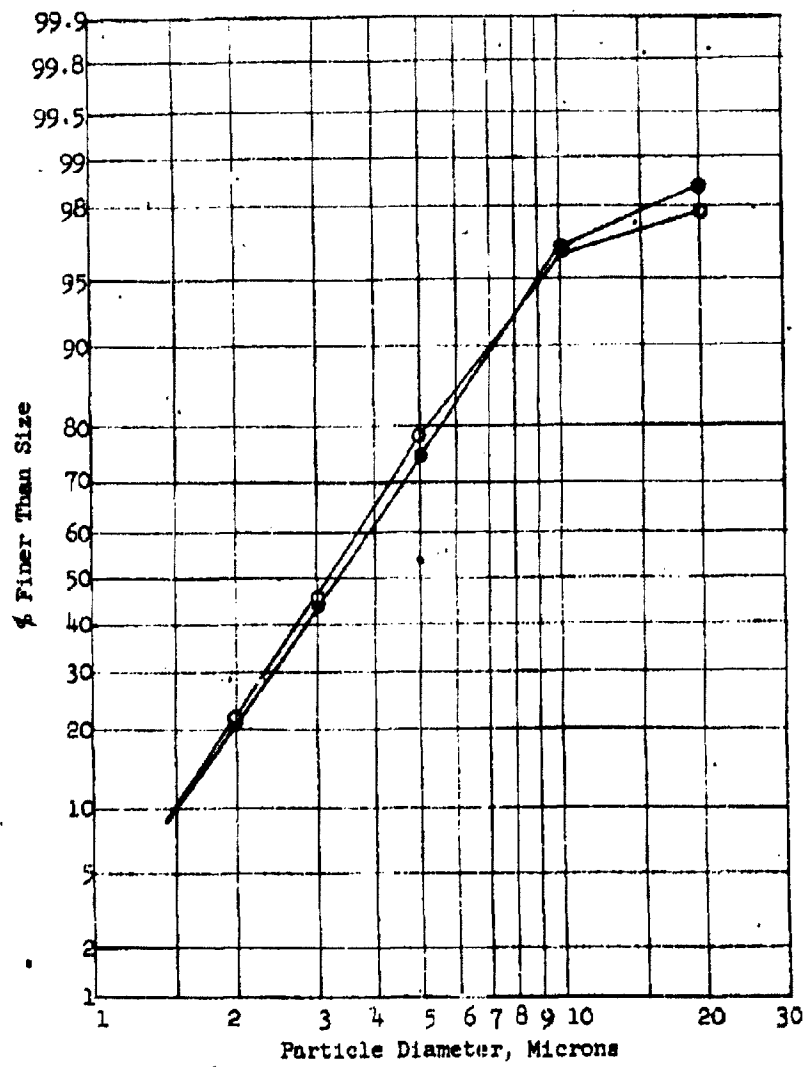


FIGURE 4.4.1
DUPLICATE SIZE ANALYSES ON SM SAMPLE GBL/B-0807006

	MMD	OSU	$\% < 2\mu$
# I	3.3μ	1.84	75.0
# II	3.2μ	1.83	78.2

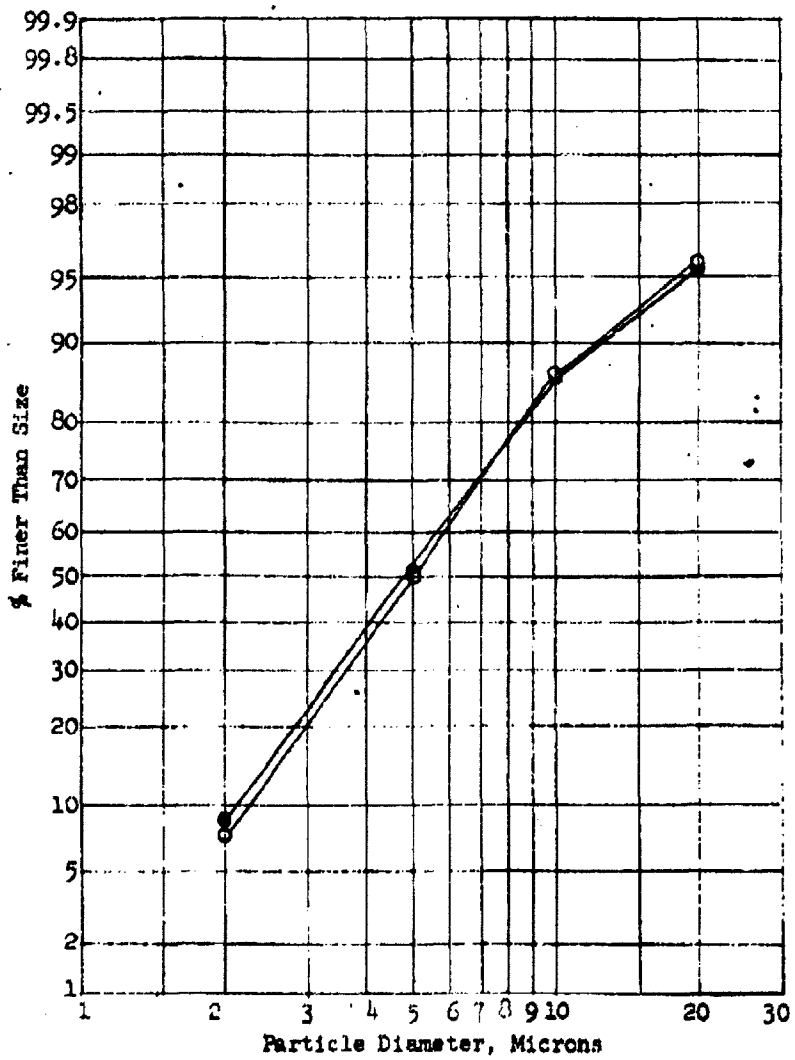


FIGURE 4.4.2
DUPLICATE SIZE ANALYSES ON SM SAMPLE OBL#A-3416554

I ● $\frac{MMD}{4.6\mu}$ $\frac{GSD}{1.92}$ $\frac{\% \text{ finer}}{52}$
 # II ○ $\frac{5.0\mu}{}$ $\frac{1.85}{}$ $\frac{50}{}$

Page determined to be Unclassified
 Reviewed Chief, RDD, WHS
 IAW EO 13526, Section 3.5
 Date: MAY 17 2013

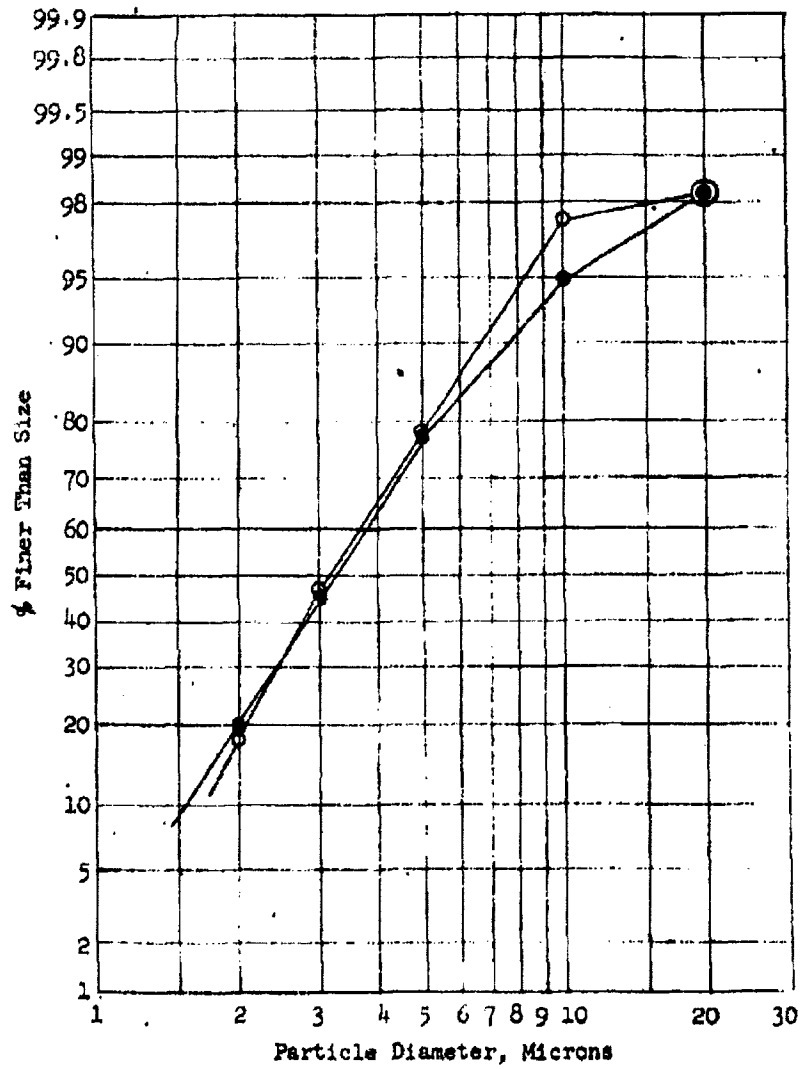


FIGURE 4.4.3
DUPLICATE SIZE ANALYSES ON SM SAMPLE G3L#A-3416691

MMD	GSD	$\% < 5\mu$
# I ● 3.25μ	1.82	77.6
#II ○ 3.15μ	1.80	78.6

NOTE: Duplicate size analyses were run on individual samples.

- 65 - Page determined to be Unclassified

Reviewed Chief, RDD, WHS

IAW EO 13526, Section 3.5

Date:

MAY 17 2013

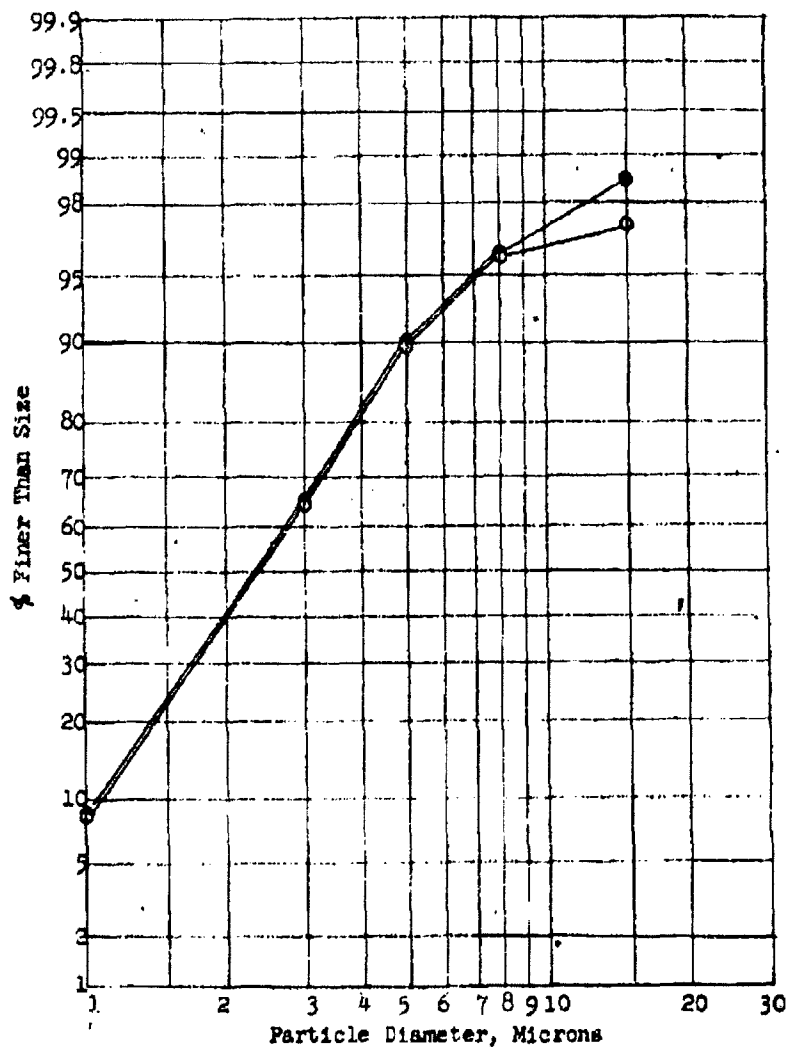


FIGURE 4.4.4
CENTRIFUGE SIZE DISTRIBUTION FOR TALC

MD	SD	$\% < 5 \mu$
# I \bullet 2.30μ	1.84	90.7
# II \circ 2.37μ	1.84	89.8

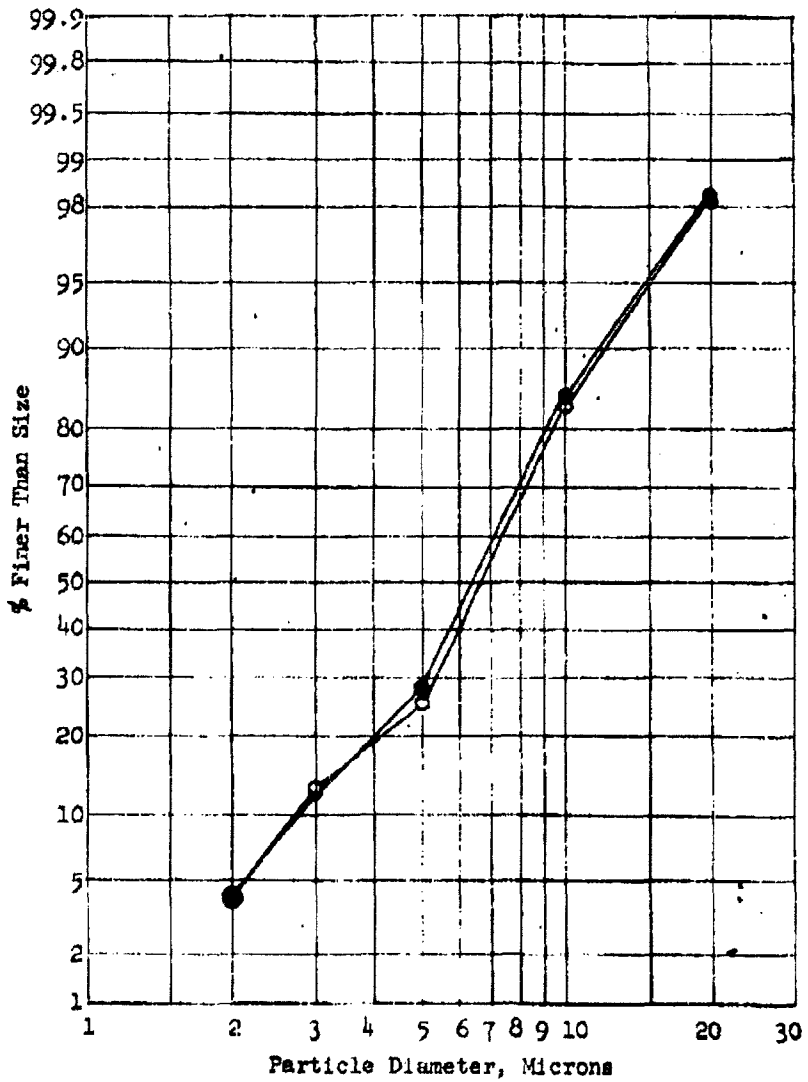


FIGURE 4.4.5
CENTRIFUGE SIZE ANALYSIS FOR GMI "JET" FLOUR

	MMD	GSD	% 5μ
# I ●	6.45μ	1.62	28.3
# II ○	6.65μ	1.72	25.4

The analysis of the Mistron No. 18 talc (Figure 4.4.4) gave values of the MMD of 2.30 and 2.37 microns, with approximately 90% less than 5 micron diameter.

Figure 4.4.5 gives the values for the General Mills "Jet" flour, which was found to have an average MMD value of 6.55 microns.

The materials covered in these particle size determinations have been used in the experiments on feeding concepts and deagglomeration by aerodynamic forces.

~~CONFIDENTIAL~~

5. STUDIES OF THE AERODYNAMIC CHARACTERISTICS OF WING-MOUNTED EXTERNAL AIRCRAFT STORES

Installation of external BW disseminator stores on the delivery aircraft will result in a reduction in its performance capabilities. An evaluation of the effects of the external store installation is therefore an important part of this study. The aerodynamic drag caused by the store installation is a very important consideration, since it will define the increase in thrust required to maintain a given flight speed or the reduction in speed which will occur with a given available thrust.

The incremental drag that is imposed on an aircraft wing by an externally mounted store arises from two main sources. The first is the isolated store drag (the drag of the store itself) and the second is the contribution to the incremental drag from the interference effects that arise when the store is installed on the aircraft wing. Since both of these contributions are of significant magnitude, and the interference drag contribution is strongly dependent on the details of the installation, simple, general solutions for this problem do not exist. The most useful available data are believed to be those from the systematic investigations of specific store installations.

5.1 Installed External Store Data

A comprehensive investigation of this subject was conducted by Spreemann and Alford.^{5.1.1} This investigation was made in the Langley high-speed 7-ft by 10-ft tunnel through a Mach number range of 0.41 to 0.96 to determine the effects of external-store fineness ratio, store shape, store

5.1.1 Spreemann, K.P. and W.J. Alford, "Investigation of the Effects of Geometric Changes in an Underwing Pylon-Suspended External-Store Installation on the Aerodynamic Characteristics of a 45 Degree Sweepback Wing at High Subsonic Speeds." NACA Research Memorandum RM 150112, 1951

~~CONFIDENTIAL~~

DECLASSIFIED IN FULL

Authority: EO 13526

Chief, Records & Declass Div, WHS

Date: MAY 17 2013

~~CONFIDENTIAL~~

chordwise position, pylon thickness, pylon length, and pylon sweep angle on the aerodynamic characteristics of several underwing pylon-suspended external stores in combination with a 45 degree sweptback semispan wing and fuselage. The store profiles corresponded to NACA 65A-series bodies of revolution, the pylons were NACA-65A series airfoil sections, and the wing was an NACA 65A006 airfoil section.

The coordinates for NACA 65A-series bodies of revolution of various fineness ratios are given in Figure 5.1.1.

Values of the incremental drag coefficient based on wing area, C_{Dg} , are given in Reference 5.1.2. However, it is considered preferable in our studies of EW stores to adopt a definition based on volume to the 2/3 power, as used by Heaslet and Nitzberg^{5.1.2}, since the volume of the store is an important variable in our analyses. This definition is:

$$C_{Dv} = \frac{D}{1/2 \rho_0 U_0^2 (V)^{2/3}}$$

where D = incremental drag of store, pounds

ρ_0 = air density in the free stream, slugs/ft³

U_0 = velocity in the free stream, ft/sec

V = volume of the store, ft³

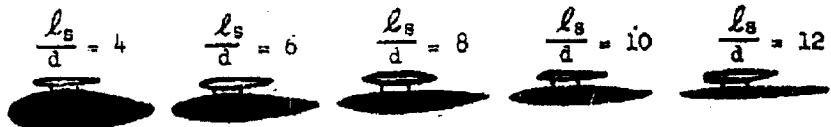
This drag coefficient, C_{Dv} , may be obtained from values of the drag coefficient based on wing area, C_{Dg} as follows:

5.1.2 Heaslet, M. A. and G. E. Nitzberg, "The Calculation of Drag for Airfoil Sections and Bodies of Revolution at Subcritical Speeds", NACA Research Memorandum RM No. A7B06, 1947.

~~CONFIDENTIAL~~

DECLASSIFIED IN FULL
Authority: EO 13526
Chief, Records & Declass Div, WHS
Date:

MAY 17 2013



Station	Radius	Radius	Radius	Radius	Radius
0	0	0	0	0	0
.5	1.92	1.28	.96	.76	.64
.75	2.32	1.54	1.16	.92	.78
1.25	2.96	1.98	1.48	1.18	.98
2.5	4.06	2.70	2.02	1.62	1.36
5.0	5.46	3.64	2.72	2.18	1.82
7.5	6.62	4.42	3.32	2.66	2.22
10.0	7.60	5.06	3.80	3.04	2.54
15.0	9.14	6.10	4.58	3.56	3.06
20.0	10.32	6.88	5.16	4.12	3.44
25.0	11.20	7.48	5.60	4.48	3.74
30.0	11.86	7.90	5.92	4.74	3.96
35.0	12.28	8.18	6.14	4.92	4.10
40.0	12.48	8.32	6.24	5.00	4.16
45.0	12.46	8.30	6.22	4.98	4.16
50.0	12.16	8.10	6.08	4.86	4.06
55.0	11.58	7.72	5.80	4.64	3.86
60.0	10.76	7.18	5.38	4.30	3.60
65.0	9.74	6.50	4.88	3.90	3.26
70.0	8.58	5.72	4.30	3.44	2.86
75.0	7.28	4.86	3.64	2.92	2.42
80.0	5.88	3.92	2.94	2.36	1.96
85.0	4.42	2.96	2.22	1.78	1.48
90.0	2.98	1.98	1.48	1.18	1.00
95.0	1.52	1.00	.76	.60	.50
100.0	.06	.04	.02	.02	.02
L.E. rad.	1.60	1.06	.80	.64	.54
T.E. rad.	.06	.04	.02	.02	.02

Source: Reference 5.1.1

FIGURE 5.1.1 ORDINATES, IN PERCENT LENGTH, FOR FIVE NACA 65A-SERIES BODIES OF REVOLUTION USED AS EXTERNAL STORES

$$C_{Dy} = C_{Ds} \left[\frac{S}{V^{2/3}} \right]$$

where S is the wing area (0.125 ft² or 18 in²).

The volume of the NACA-65A series body of revolution was obtained from the data given in Reference 5.1.1 by graphical integration. For a store with a length-to-diameter ratio, ℓ_s/d , of 8, the total volume of one store is 0.835 in³. The general relationship for calculation of the volume of an NACA 65A-series body with $\ell_s/d = 8$ is $V = 0.0067 \ell_s^3$. Since the experiments discussed in Reference 5.1.1 were conducted with one store mounted on a semispan model wing with an area of 9.0 in², C_{Dy} becomes

$$C_{Dy} = C_{Ds} \left[\frac{9.0}{0.835)^{2/3}} \right] = 10.15 C_{Ds}$$

Typical values of the drag coefficients from Reference 5.1.1 are tabulated below for the case of a store of fineness ratio $\ell_s/d = 8$, mounted on a pylon with a length*-to-chord ratio $\ell_p/C = 0.0945$ (with zero degree sweep angle) at values of the lift coefficient, C_L , of zero and 0.3.

<u>Mach Number</u>	<u>$C_L = 0$</u>		<u>$C_L = 0.3$</u>	
	<u>C_{Ds}</u>	<u>C_{Dy}</u>	<u>C_{Ds}</u>	<u>C_{Dy}</u>
0.50	0.0040	0.0406	0.0070	0.0710
0.80	0.0065	0.0660	0.0085	0.0863
0.92	0.0170	0.1726	0.0185	0.1876

For the above cases, the angle of attack, α , at $C_L = 0$ was approximately 0.5 degrees and at $C_L = 0.3$ was approximately $\alpha = 5.5$ degrees. The Reynolds

* The pylon length is defined as the distance between parallel tangents to the lower surface of the wing and the upper surface of the store.

~~CONFIDENTIAL~~

number, N_R , based on the mean aerodynamic chord of the wing, varied as follows:

At $M = 0.50$, N_R varied from 0.55 to 0.60×10^{-6}

At $M = 0.80$, N_R varied from 0.70 to 0.75×10^{-6}

At $M = 0.92$, N_R varied from 0.72 to 0.77×10^{-6}

A more complete presentation of this drag information is given in Figures 5.1.2 and 5.1.3, which show the drag coefficient versus Mach Number for several configurations at two values of the lift coefficient. Conversion of values of C_{Dg} to C_{Dy} were performed in the same manner as illustrated above for the case where $l_s/d = 8$.

In addition to the values from Reference 5.1.1, Figures 5.1.2 and 5.1.3 present values from Reference 5.1.3 (Bielat and Harrison) and Reference 5.1.4 (North American Aviation, Inc.).

From Reference 5.1.3, values were obtained for a body with a cylindrical center section. This body had an ogival nose and tail section each 4 inches long and a cylindrical center section 6.27 inches in length. The body diameter was 1.50 inches. This gives an l_s/d equal to 9.31.

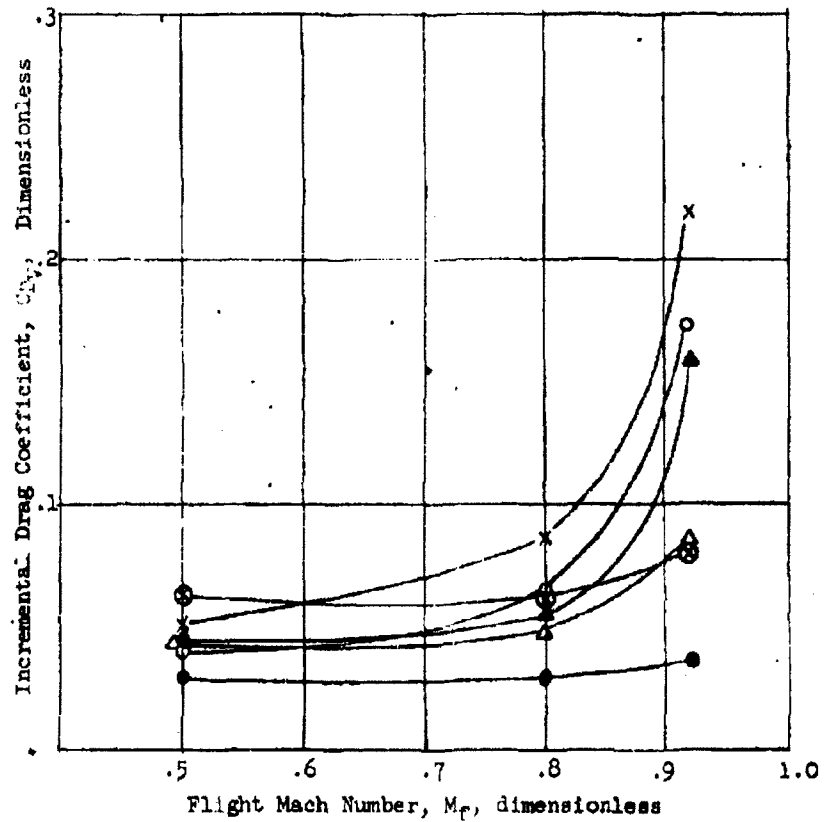
The body volume was obtained in a manner similar to that outlined previously and is equal to 18.22 cu in.

The values of C_{Dy} for various Mach numbers were obtained by using a wing area of 165 sq in. Therefore, the relationship between C_{Dy} and C_{Dg} is given as follows:

$$C_{Dy} = C_{Dg} \left[\frac{S}{V^{2/3}} \right]$$

5.1.3 Bielat, R. P. and D. E. Harrison, "A Transonic Wind-Tunnel Investigation of the Effects of Nacelle Shape and Position on the Aerodynamic Characteristics of Two 47-Degree Sweptback Wing-Body Configurations", NACA RM L52G02, 1952

5.1.4 North American Aviation, Inc. Report No. NA-60-1403 (Secret) Nov., 1960.



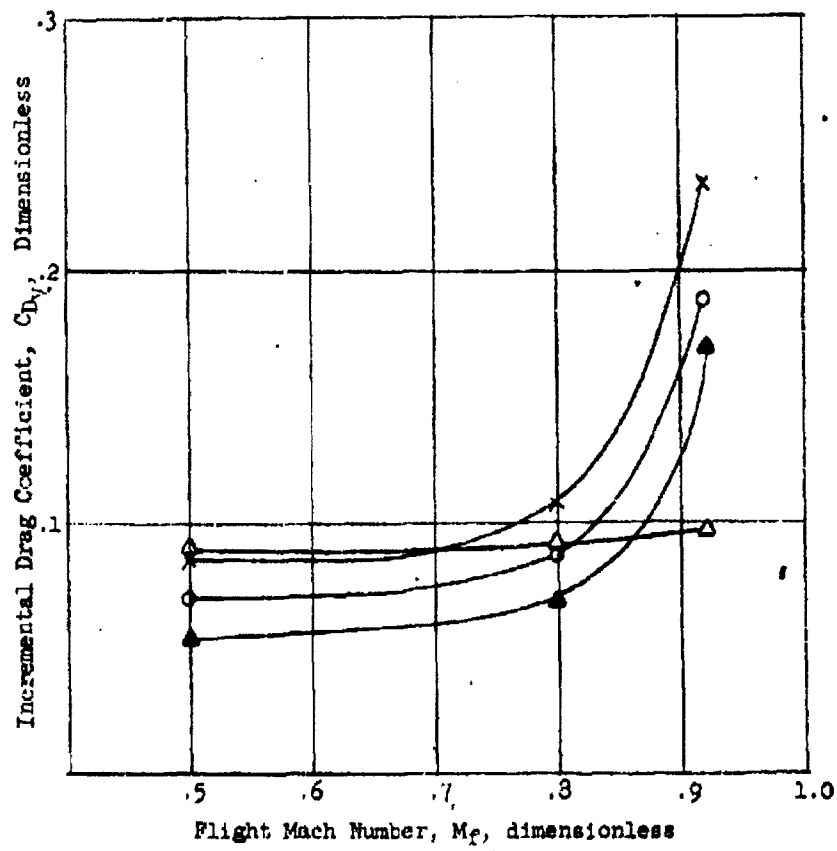
$\times = l_s/d = 6$ } NACA-65A Series,
 $\circ = l_s/d = 8$ } Bodies of Revolution, (RML50LM)
 $\blacktriangle = l_s/d = 10$
 $\triangle = l_s/d = 9.51$ Cylindrical Center Section, Forward Swept Pylon (RML52CX)
 $\bullet = l_s/d = 9.51$ Isolated Nacelle (RML52CO)
 $\otimes =$ Proposed 150 Gal BW Store - North American Aviation
 Dwg. No. 2521-900C01

NOTES:

(1) ... is based on $(\text{Volume})^{2/3}$

(2) All data at lift coefficient, $C_L = 0$.

Figure 5.1.2 Incremental Drag Coefficient Versus Flight Mach Number for Various External Store Configurations at Zero Lift Coefficient



$\times = l_s/d = 6$ } NACA-65A Series
 $\circ = l_s/d = 8$ } Bodies of Revolution, (ML50L12)
 $\blacktriangle = l_s/d = 10$
 $\triangle = l_s/d = 9.5$ Cylindrical Center Section, Forward Swept
 Pylon (ML52GC2)

NOTES:

(1) $C_{D\Delta}$ is based on $(Volume)^{2/3}$

(2) All data at lift coefficient, $C_L = 0.3$

Figure 5.1.3 Incremental Drag Coefficient Versus Flight Mach Number for Various External Store Configurations at Lift Coefficient (C_L) of 0.3

where

$$\frac{S}{\sqrt{2}/3} = \frac{165}{13.82} = 11.91$$

The resulting drag coefficient values are tabulated below:

Mach Number	<u>$C_L = 0$</u>		<u>$C_L = .3$</u>	
	<u>C_{D_S}</u>	<u>C_{D_V}</u>	<u>C_{D_S}</u>	<u>C_{D_V}</u>
.5	.0035	.0417	.0075	.0893
.8	.0040	.0476	.0075	.0893
.92	.0070	.0834	.0080	.0953

The pylon length-to-chord ratio, $\ell_p/c = 63.5\%$ (approx. 75° swept forward).

Reference 5.1.3 also gives the drag coefficient for isolated nacelles as determined from unpublished rocket data. The values of C_{D_S} were based on the wing area of the model or 165 in^2 .

The values of C_{D_S} and C_{D_V} are tabulated below:

Mach Number	<u>C_{D_S}</u>	<u>C_{D_V}</u>
0.50	0.0025	0.0298
0.80	0.0025	0.0298
0.92	0.0030	0.0357

A method for calculating the drag coefficient C_{D_S} of an isolated body of revolution is presented by Heaslet and Nitzeberg.^{5.1.2} To apply the method it is necessary to know the velocity and boundary layer thickness distribution of the air flow around the body of revolution, and also the Mach number of the free stream transition point from laminar to turbulent flow and the Reynolds number based on the axial length. Spreemann and Alford^{5.1.1} used the Heaslet and Nitzeberg^{5.1.2} method to calculate the isolated store drag for their NACA 65A-series bodies of revolution. A value of C_{D_S} of 0.0035 was obtained for a store having $\ell_s/d = 8$ at a Mach Number of 0.8.

~~CONFIDENTIAL~~

The store which is considered in Reference 5.1.4 is 220 inches long, 25 inches in diameter ($\ell_s/d = 8.8$) with a volume of 43.36 ft^3 and a plan area of 31.4 ft^2 .

The reported values of the drag coefficient for this store were based on the plan area of the store. These values were converted to C_{Dv} for purposes of comparison, and are tabulated below:

Mach Number	Reported Drag Coefficient	C_{Dv}
0.50	0.0245	0.062
0.80	0.0245	0.062
0.92	0.0315	0.080

~~CONFIDENTIAL~~

DECLASSIFIED IN FULL
Authority: EO 13526
Chief, Records & Declass Div, WHS
Date:

MAY 17 2013

~~CONFIDENTIAL~~

5.2 Discussion of Aerodynamic Data

Figures 5.1.2 and 5.1.3 show that the drag coefficients for most store installations increase substantially at high subsonic Mach numbers. These increases are quite pronounced in the Mach number range (0.7 to 0.9) of primary interest in this study. The increase in drag coefficient of the NACA 65A-series stores above Mach 0.7 is caused primarily by interference effects.

The importance of the interference drag contribution is apparent when we compare the drag coefficients for the store installations with that of the isolated nacelle.

Parameters which affect the interference drag are store fineness ratio, store shape, pylon length, thickness and sweep angle, and the position of the store both chordwise and spanwise on the wing. Spreemann and Alford^{5.1.1} concluded that the sweep angle is a very important variable and that it is desirable to place the store either extremely far forward or aft on the wing chord. The benefits of forward sweeping of the pylon are illustrated in Figure 5.1.2 which shows a reduction in incremental drag at $M_f = 0.9$ of approximately 50% for this case.

Figures 5.1.2 and 5.1.3 indicate that there is no serious departure from a nominal incremental drag coefficient when a cylindrical center section is used instead of a smooth NACA-65A series body of revolution. A store configuration of this type is currently used for standard subsonic aircraft stores. The coordinates of this shape are shown in Figure 5.2.1.

5.2.1 U. S. Air Research and Development Command. ARDCM-80-1. Handbook of Instructions for Aircraft Designers. Tenth Edition, 1958.

~~CONFIDENTIAL~~

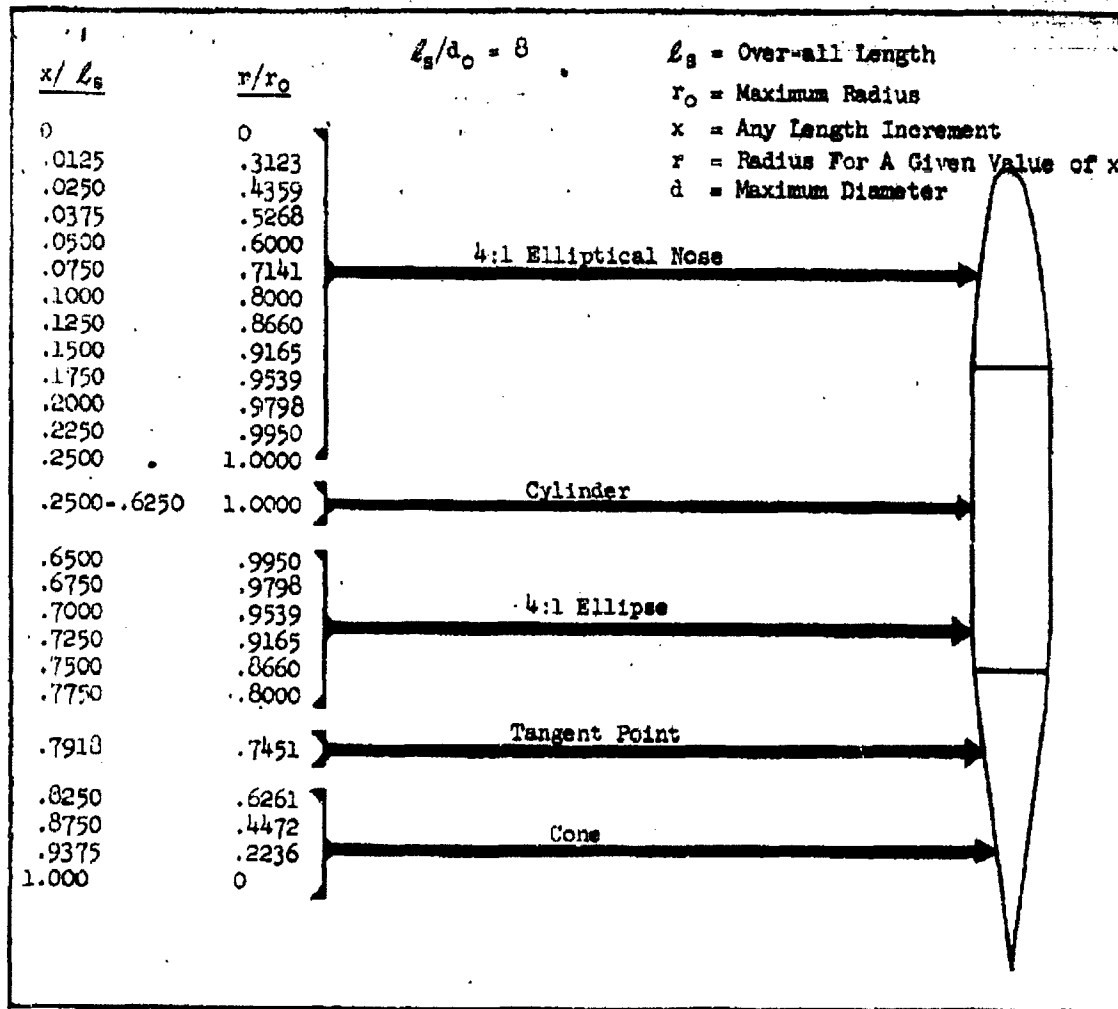


Figure 5.2.1 Shapes Definition, Subsonic External Store

~~CONFIDENTIAL~~

The final choice of a store shape and fineness ratio will depend on the detailed limitation on the installation such as clearance and center of gravity considerations. However, it is believed that the data reported in this section will serve as important guidelines in the later design studies.

- 80 -

~~CONFIDENTIAL~~

DECLASSIFIED IN FULL

Authority: EO 13526

Chief, Records & Declass Div, WHS

Date:

MAY 17 2013

6. INVESTIGATIONS OF PROPERTIES OF SLURRIES

6.1 Properties of Egg Slurries

In order to provide design data for liquid agent dissemination systems, we have initiated work to experimentally determine the density, viscosity, heat capacity and thermal conductivity of egg slurries.

In this reporting period, measurements of density and viscosity have been made. Special apparatus will be required for the thermal property measurements.

Four frozen egg slurry samples were received from Fort Detrick for this work. These were designated as W.E.S. #1, #2, #3 and #4. They were uninfected whole-egg slurries which had been purified, to different degrees, in the preparation process.

Since some of the samples were Non-Newtonian, it was necessary to collect data for consistency curves, rather than make conventional viscosity measurements. These data were collected by evaluating the sample in a modified* Stormer viscometer, which is equipped with a closely controlled constant temperature bath. The least viscous sample (W.E.S. #4) was evaluated using an Ostwald (orifice-type) viscometer.

The data obtained for these samples are summarized below:

1. Sample W.E.S. #1, analyzed in the Stormer viscometer, was found to be Newtonian within a shear rate range of 70.4 to 363.5 cm/sec-cm at 20°C. The absolute viscosity of this slurry was found to be 25.1 centipoises. The density of this slurry is 1.0304 gm/cm³ at 20° centigrade.

*These modifications are described by E. K. Fischer in "Colloidal Dispersions" John Wiley and Sons, Inc., New York, 1950. Application of the modified Stormer Viscometer is discussed by S. P. Jones in the Journal of Colloid Science, Vol. 7, No. 3, June 1952, p. 272-283.

2. Sample W.E.S. #2, also analyzed in the Stormer viscometer, was found to be Non-Newtonian. Tests were made at 20°C in a shear rate range of 214 to 433 cm/sec-cm. Following are the values of apparent viscosity of this slurry, at the stated shear rates.

<u>Shear Rate, cm/sec-cm</u>	<u>Apparent Viscosity, Centipoises</u>
214	8.4
352	10.3
433	12.7

The density of this slurry was 1.0210 gm/cm³ at 20°C. The curve of shear rate versus shear stress is compared with that for sample W.E.S. #1 in Figure 6.1.1.

3. Sample W.E.S. #3. An effort was made to determine the viscosity of this slurry on both the Ostwald and Stormer viscometers. Meaningful measurements were not obtainable. This slurry contained solids which clogged the Ostwald viscometer. The viscosity was also found to be too low to be properly handled on the Stormer viscometer.

The density of this sample was found to be 1.0006 gm/cm³ at 20°C.

4. Sample W.E.S. #4 was analyzed with the Ostwald viscometer. It was found to have a viscosity of 1.12 centipoises and a density of 1.0012 gm/cm³. This sample had been purified by a Freon process and had properties very nearly equal to those of water.

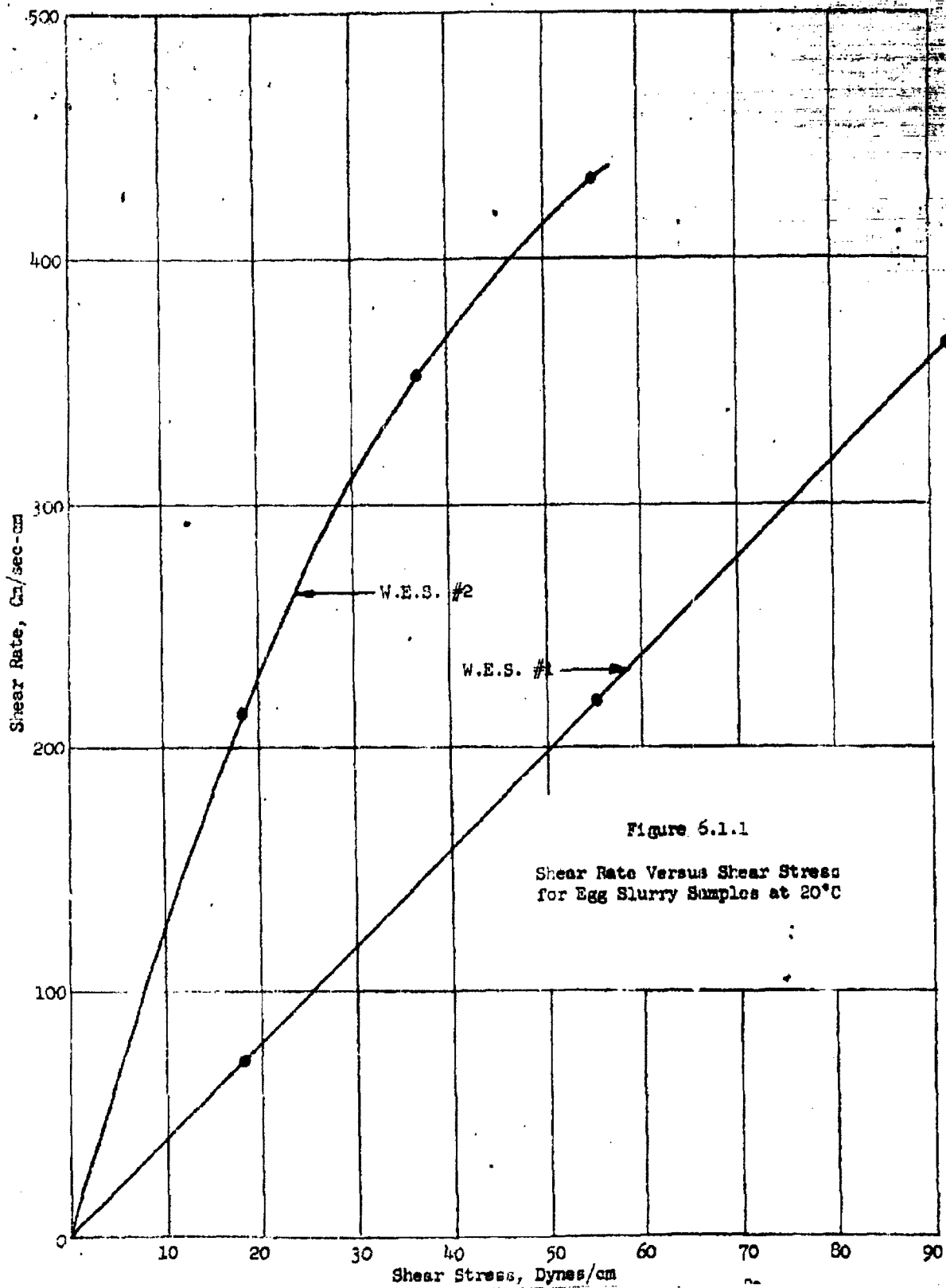


Figure 6.1.1

Shear Rate Versus Shear Stress
for Egg Slurry Samples at 20°C

~~CONFIDENTIAL~~

6.2 Properties of Slurries of SM in Inert Fluorochemical Liquid

The possibility of disseminating normally dry BW agents by suspending them in an inert liquid has been considered. This approach could substantially reduce the problem of feeding the agent to the point of discharge at a uniform rate.

Of the several technical problems involved in this approach, the weight penalty incurred by adding the liquid is perhaps the most apparent.

A series of experiments has therefore been initiated to determine the physical characteristics of such slurries, as a function of the concentration of solids.

Slurries of SM simulant in Minnesota Mining Fluorochemical FC-75 are being studied. The compatibility of this liquid with Biological Agents is currently being studied at Fort Detrick. Good compatibility is indicated.

Some of the properties of FC-75 are as follows:

Density gm/cc: 1.77

Specific Heat Cal/gm: 0.248 at 25°C

Boiling Point: 95% minimum between
99 and 107°C.

Concentrated slurries of SM in FC-75 are non-Newtonian and have a high apparent viscosity. Figure 6.2.1 shows the effect of shear rate on the apparent viscosity of the slurries with 20 and 25 percent SM by weight. These data were obtained from tests on the modified Stormer Viscometer, equipped with a temperature control bath.

Note that the apparent viscosity is quite sensitive to the concentration of SM. For example, at a shear rate of 100 cm/sec-cm, an increase in

~~CONFIDENTIAL~~

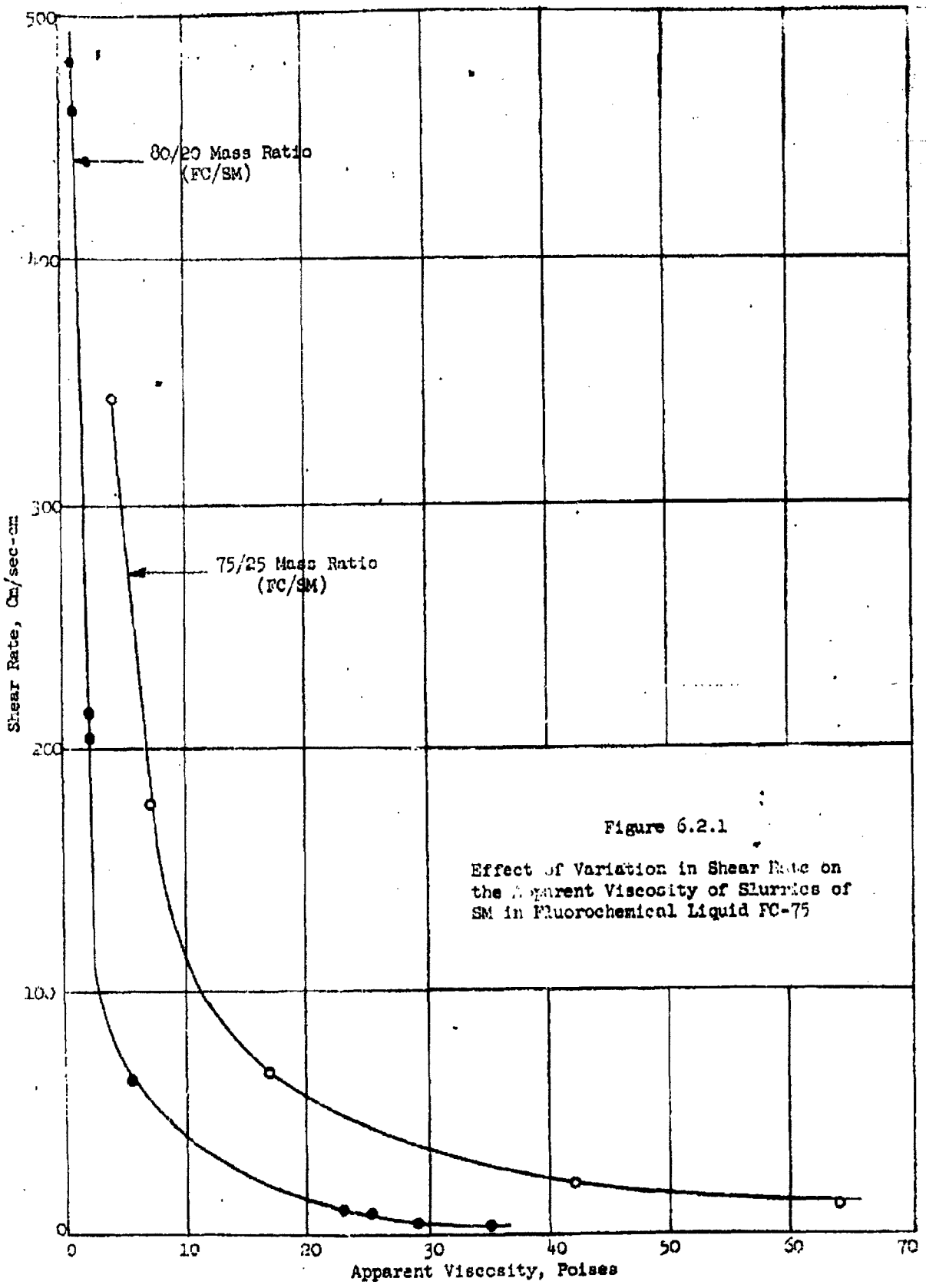


Figure 6.2.1

Effect of Variation in Shear Rate on
the Apparent Viscosity of Slurries of
SM in Fluorochemical Liquid FC-75

~~CONFIDENTIAL~~

concentration from 20 percent to 25 percent increases the apparent viscosity from approximately 2.8 poises to 11.5 poises at 20°C.

A much more detailed series of measurements is underway to explore the effects of varying concentration and temperature.

~~CONFIDENTIAL~~

7. WORK ON LIQUID AGENT DISSEMINATORS

During this reporting period, the Phase I study on an airborne line-source dissemination system was completed. This work was performed by North American Aviation, Inc., under a subcontract from General Mills, Inc.

The technical report covering this work was submitted in November 1960. This report is designated as North American Aviation Report No. NA-60-1403, dated 4 Nov. 1960, and is classified SECRET.

At the end of the Phase I study, the status of work leading to the design and manufacture of a research prototype external store for dissemination of liquid BW agents, may be summarized as follows:

1. An extensive study has been made of the capabilities (for carrying external stores) of a large number of operational aircraft, and the characteristics of acceptable stores have been established.
2. Studies of factors influencing optimum flow rate have been made and conclusions drawn.
3. Several technical problems including temperature control, anti-icing requirements and effects of the local flow fields have been studied and promising approaches to the solution of these problems have been found.

The reader is referred to the above mentioned technical report for the details of this Phase I study.

~~CONFIDENTIAL~~

8. SUMMARY AND CONCLUSIONS

During this reporting period experiments were made on feeding of dry powders by screw feeding devices and piston-type feeders (Section 2).

The experiments with screw feeders explored the delivery characteristics of two helical screw configurations. One of these had a closed-center design and the other was an open "ribbon"-type. These experiments pertained to the use of a very large screw which occupies the full diameter and length of an external store. Both configurations were found to have reproducible delivery characteristics. The delivery rate of these devices decreases as the contained material is discharged, so that a programmed increase in rotational speed is required for constant average mass-flow versus time.

Investigations of the effect of exposing the SM simulant to atmospheres with different relative humidities were made. It was found that exposure of the SM to 5% relative humidity increased the residual material in the screw, due to attractive forces which were attributed to electrostatic charging.

The experiment on feeding of Sierra Mistron No. 18 talc with a piston device indicates that the compressive stresses are below the level which will appreciably increase the bulk density of the material.

Several studies were made in the field of dissemination and deagglomeration (Section 3). Generation of aerosols by erosion was explored. Models formed by compacting finely divided powder were exposed to air flow at velocities near sonic speed. It was found that aerosols could be generated by this method, at significant mass flow rates. However, fluctuations in the flow rates were found and it appears that very close control of the preparation of the powder would be required to give adequate control of flow rate.

~~CONFIDENTIAL~~

Experiments with suspensions of powder in liquid carbon dioxide indicated that the powder can be totally aerosolized if the concentration is kept below 1 part solids in 4 parts liquid. The principal factors against this approach are the weight penalties due to the liquid and the required pressure vessel.

A piston type powder feeding device has been installed on the test section of the high-subsonic blow-down wind tunnel and initial experiments have been made. The number of large agglomerates in the generated aerosol was found to decrease when the Mach number was increased from 0.6 to 0.8. A much more detailed investigation along these lines is planned.

The characteristics of finely divided dry materials have been studied theoretically and experimentally (Section 4). The theoretical study deals with static load transmission in particulate packings. Force transmission was analyzed for granular packings and regular packings with square and hexagonal arrays, and general equations were derived.

Experiments were conducted dealing with translation of particles above a moving piston, which showed that vertical motion of a piston in a bed of relatively large elastic particles causes a complex pattern of horizontal and vertical translation. Studies of gravity flow of such particles indicated that the velocity of flow by gravity is strongly affected by local conditions. Measurements of the torque required to rotate a helical screw surrounded by powder showed that this test sharply distinguished between talc and poly vinyl alcohol powder.

~~CONFIDENTIAL~~

~~CONFIDENTIAL~~

Studies of the aerodynamic characteristics of external pylon-mounted stores were made (Section 5) which showed that data on the incremental drag coefficients from several sources agreed quite well, when reduced to a common basis, i.e., that of the $(\text{volume})^{2/3}$ of the external store. The magnitude of the interference drag contribution was found to be very important, particularly at the highest subsonic speeds. The pylon design is an important consideration in minimizing this interference drag contribution. The sources of data used show that forward or rearward swept designs are best.

The properties of slurries were studied experimentally (Section 6). These included measurements of the viscosity and density of uninfected egg slurry samples and also an initial evaluation of the variation of apparent viscosity of slurries of SM in an inert fluorochemical liquid. The experiments on egg slurries showed that the sample designated as W.E.S. #4, which had been purified by Freon, had properties nearly equal to those of water, while the other samples were considerably more viscous. The measurements on the SM slurries showed that concentrations of 20 to 25 percent solids resulted in non-Newtonian behavior. The apparent viscosity is strongly dependent on concentration.

The Phase I studies on liquid agent dissemination (Section 7) are covered in a separate report issued by North American Aviation, Inc., designated as Report No. NA-60-1403.

APPENDIX A

PROCEDURE FOR CALCULATION OF TIME SCHEDULES FOR WHITBY* CENTRIFUGE PARTICLE SIZE ANALYSIS TECHNIQUE

The time durations for gravity sedimentation periods and centrifuge operating periods in this size analysis method are calculated by the equations given below.

1. Gravity Sedimentation Period

The gravity settling time is calculated from the usual form of Stokes' Law:

$$t_g = \frac{(18 \times 10^8 \eta_0 h)}{(\rho - \rho_0) g d^2} \quad (1)$$

where t_g = time (seconds) for a particle to settle a distance h under the influence of gravity

d = particle diameter (microns)

h = settling height (centimeters) (10 cm for all tubes)

ρ = true density of particles (gm/cc).

ρ_0 = density of sedimentation liquid (gm/cc)

η_0 = absolute viscosity of sedimentation liquid (poise)

g = gravitational constant

$$\text{if we let } K_g = \frac{18 \times 10^8 \eta_0 h}{(\rho - \rho_0) g} \quad (2)$$

then Equation (1) becomes

$$t_g = \frac{K_g}{d^2} \quad (3)$$

* Whitby, K. T. ASHAE Journal Section, Heating, Piping and Air Conditioning, January 1955 (page 231) and June 1955 (pages 139-45)

2. Centrifuge Operating Period

Centrifuge settling times are calculated from a form of Stokes' law for a centrifugal field, which is derived as follows:

If we let (r) represent the radius of rotation of a particle of mass (m) rotating about an axis at an angular velocity (ω), at equilibrium, two forces will be acting on the particle, a centrifugal force and a frictional force, the latter determined by Stokes' law. Equating these forces we obtain:

$$3\pi\eta_0 a \left(\frac{dr}{dt}\right) \times 10^8 = m\omega^2 r$$

The effective mass of a spherical particle in a liquid is:

$$m = \left(\frac{\pi}{6}\right) d^3 (\rho - \rho_0)$$

therefore: $\frac{dr}{dt} = \frac{(\rho - \rho_0) \omega^2 d^2 r}{18 \times 10^8 \eta_0}$

Integrating between the starting radius (r_1), and the final radius (r_2), we obtain:

$$t_c = t_2 - t_1 = \frac{18 \times 10^8 \eta_0}{(\rho - \rho_0) \omega^2 d^2} \log_e \left(\frac{r_2}{r_1} \right) \quad (4)$$

where

t_c = the centrifuge time required to centrifuge a particle of size d from r_1 to r_2 .

K values may also be defined from Equation 4 for predetermined centrifuge speeds. If K_s represents the K value associated with a given centrifuge speed s , then:

$$K_s = \frac{18 \times 10^8 \eta_0}{(\rho - \rho_0) \omega_s^2} \quad (5)$$

then Equation 4 becomes:

$$t_c = \left(\frac{K_s}{d^2}\right) \log_e \left(\frac{r_2}{r_1}\right) \quad (6)$$

r_2 in Equation 6 is constant for any specific centrifuge apparatus, but r is dependent upon the radius of the top of the tube and distance which the particle has already settled under the influence of gravity; therefore:

$$r_1 = r_0 + 10 \left(\frac{t_g}{t_{cg}}\right) \quad (7)$$

where:

t_g = time for last gravity particle size d_g to settle 10 cm under gravity

t_{cg} = time for first centrifuge particle size d_c to settle 10 cm under gravity

r_0 = starting radius of all particles in the feeding layer at $t = 0$

Substituting Equation 3 into Equation 7, we obtain:

$$r_1 = r_0 + 10 \left(\frac{d_c^2}{d_g^2}\right) \quad (8)$$

Since r_1 is a function of the last gravity size and the centrifuge size under consideration, it is simple to calculate the centrifuge portion of the run from a tabulation of values of a constant, Q , which is a function of d_g and d_c , as shown below:

From Equation 6, let us define Q as:

$$Q = \left(\frac{1}{d_g^2}\right) \log_e \left(\frac{r_2}{r_1}\right) \quad (9)$$

then

$$t_c = K_s Q \quad (10)$$

Substituting Equation 8 into Equation 9 yields:

$$Q = \left(\frac{1}{d_c^2} \right) \log_e \left[\frac{r_2}{r_0 + 10 \left(\frac{d_c^2}{d_g^2} \right)} \right] \quad (11)$$

A table of Q values may be computed from Equation 11 for any centrifuge system having constant r_0 and r_2 values.

Since centrifuge size analysis runs are of short duration, the starting-stopping correction makes up a major portion of the running time. This necessitates an accurate determination of the starting-stopping correction. This is accomplished by means of a stroboscope to obtain accurate angular velocity-time measurements which are plotted as angular velocity squared (ω^2) versus time (t). The net correction is obtained by integrating the areas of the starting-stopping curves to obtain the net correction as follows.

$$\text{Net Correction} = \frac{\text{Area A} - \text{Area B}}{Y \text{ (to the same scale as } t)}$$

where A, B and Y are as defined in the sketch below.

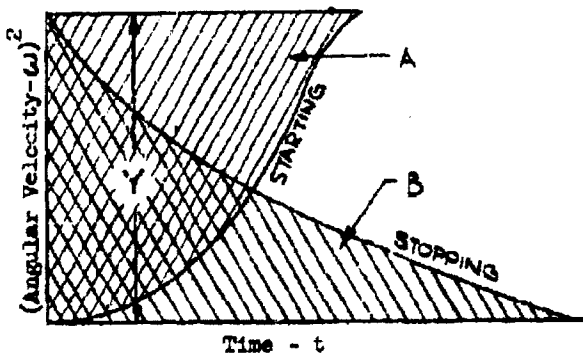


Figure A-1. Typical Starting and Stopping Curves

A-4



DEPARTMENT OF DEFENSE
WASHINGTON HEADQUARTERS SERVICES
1155 DEFENSE PENTAGON
WASHINGTON, DC 20301-1155



MEMORANDUM FOR DEFENSE TECHNICAL INFORMATION CENTER
(ATTN: WILLIAM B. BUSH)
8725 JOHN J. KINGMAN ROAD, STE 0944
FT. BELVIER, VA 22060-6218

AUG 1 2013

SUBJECT: OSD MDR Cases 12-M-3144 through 12-M-3156

At the request of [REDACTED], we have conducted a Mandatory Declassification Review of the documents in the above referenced cases on the attached Compact Disc (CD) under the provisions of Executive Order 13526, section 3.5, for public release. We have declassified the documents in full. We have attached a copy of our response to the requester. If you have any questions, please contact Ms. Luz Ortiz by phone at 571-372-0478 or by e-mail at luz.ortiz@whs.mil, luz.ortiz@osd.mil, or luz.ortiz@osdj.ic.gov.

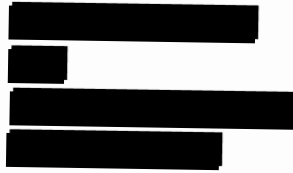
Robert Storer
Chief, Records and Declassification Division

Attachments:

1. MDR request w/ document list
2. OSD response letter
3. CD (U)



April 26, 2012



Department of Defense
Directorate for Freedom of Information and Security Review
Room 2C757
1155 Defense Pentagon
Washington, D.C. 20301-1155

Sir:

I am requesting under the Mandatory Declassification Review provisions of Executive Order 13291, copies of the following documents. I have tried several times to acquire them through DTIC, but the sites stated they are not available.

I am conducting research into the previous methods used to disseminate biological agents. Many source I use to have access to have been deleted from the internet. On numerous occasions I have been informed that formerly classified information that was declassified, have now become classified again (since 911). My attempts to locate such Executive Orders, regulations, laws, or other changes to this question have not successful nor revealed a specific source. As such I would appreciate any information you can shed on this question.

Documents requested.

AD 348405, Dissemination of Solid and Liquid BW (Biological Warfare) Agents Quarterly 12-M-3144
Progress Report Number 14, 4 Sept - 4 Dec 1963, G. R. Whitnah, February 1964, General Mills
Report number 2512, General Mills, Inc., Minneapolis, MN, Contract number DA 18064 CML
2745, 102 pages. Prepared for U.S. Army Biological Laboratories, Fort Detrick, Maryland.
Approved by S.P. Jones, Director of Aerospace Research at General Mills. Project No. 82408.
General Mills Aerospace Research Division, 2295 Walnut Street, St. Paul 13, Minnesota.

AD 346751, Dissemination of Solid and Liquid BW (Biological Warfare) Agents, Quarterly 12-M-3145
Progress Report Number 12, March 4 - June 4, 1963, G. R. Whitnah, July 1963, General Mills
Report number 2411, General Mills, Inc., Minneapolis, MN, Contract number DA 18064 CML
2745. 184 pages. Approved by S.P. Jones, Director of Aerospace Research at General Mills.
Project No. 82408. General Mills Aerospace Research Division, 2295 Walnut Street, St. Paul 13,
Minnesota.

AD 346750, Dissemination of Solid and Liquid BW (Biological Warfare) Agents, Quarterly 12-M-3146
Progress Report Number 13, 4 June - 4 Sept 1962, G.R. Whitnah, October 1963, General Mills

12-M-3144

Report number 2451, General Mills, Inc., Minneapolis, MN, Contract Number DA 18064 CML 2745. 19 pages (?)

AD 332404, Dissemination of Solid and Liquid BW (Biological Warfare) Agents, Quarterly ~~12-M-3147~~
Progress Report Number 7, Dec. 4, 1961 - March 4, 1962, by G.R. Whitnah, February 1963,
General Mills Report Number 2373, General Mills, Inc., Minneapolis, MN, Contract Number
DA 18064 CML 2745. 123 pages.

AD 333298, Dissemination of Solid and Liquid BW (Biological Warfare) Agents, Quarterly ~~12-M-3148~~
Progress Report Number 9, June 4, 1962 - Sept. 4, 1962, by G.R. Whitnah, October 1962,
General Mills Report Number 2344, General Mills, Inc., Minneapolis, MN, Contract Number
DA 18064 CML 2745. 130 (or 150) pages.

AD 332405, Dissemination of Solid and Liquid BW (Biological Warfare) Agents, Quarterly ~~12-M-3149~~
Progress Report Number 8, Period March 4, 1962 - June 4, 1962. G.R. Whitnah, August 1962,
General Mills Report Number 2322, General Mills, Inc., Minneapolis, MN, Contract Number
DA 18064 CML 2745. 198 pages.

AD 329067, Dissemination of Solid and Liquid BW (Biological Warfare) Agents, Quarterly ~~12-M-3150~~
Progress Report Number Six, G.R. Whitnah, February 1962, General Mills Report Number 2264,
General Mills, Inc., Minneapolis, MN, Contract Number DA 18064 CML 2745. 103 pages.
Approved by S.P. Jones, Manager, Materials and Mechanics Research, General Mills Research
and Development Office, 2003 East Hennepin Avenue, Minneapolis 13, Minnesota.

AD 327072, Dissemination of Solid and Liquid BW (Biological Warfare) Agents, Quarterly ~~12-M-3157~~
Progress Report Number Five, 4 June - 4 Sept 1961. by G.R. Whitnah, November 1961, General
Mills Report Number 2249, General Mills, Inc., Minneapolis, MN, Contract Number DA 18064
CML 2745.

AD 325247, Dissemination of Solid and Liquid BW (Biological Warfare) Agents, Quarterly ~~12-M-3152~~
Progress Report Number 4, 4 March - 4 June 1961, by J.E. Upton for G.R. Whitnah, Project
Manager. February 1963, General Mills Report Number 2216, General Mills, Inc., Minneapolis,
MN, Contract Number DA 18064 CML 2745. General Mills Electronics Group, Research Dept.,
2003 East Hennepin Avenue, Minneapolis 13, Minnesota. 225 pages.

AD 324746, Dissemination of Solid and Liquid BW (Biological Warfare) Agents, Progress ~~12-M-3153~~
Report 3 Juuen - 3 Sept. 1960. by G.R. Whitnah, October 1960, General Mills Report Number
2125, General Mills, Inc., Minneapolis, MN, Contract Number DA 18064 CML 2745. 78 pages

AD 323599, Dissemination of Solid and Liquid BW (Biological Warfare) Agents, Quarterly ~~12-M-3154~~
Progress Report Number 2, for period 4 Sept - 4 Dec 1960, by G.R. Whitnah, February 1961,
General Mills Report Number 2161, General Mills, Inc., Minneapolis, MN, Contract Number
DA 18064 CML 2745. 90 pages? Mechanical Division of General Mills, Inc., Research
Department, 2003 East Hennepin Avenue, Minneapolis 13, Minnesota.

AD 323598, Dissemination of Solid and Liquid BW (Biological Warfare) Agents, Quarterly *12-M-3155*
Progress Report, for period 4 Dec. 1960 - 4 March 1961, by G.R. Whitnah, May 1961, General
Mills Report Number 2200, General Mills, Inc., Minneapolis, MN, Contract Number DA 18064
CML 2745. 95 pages.

AD 337635, Dissemination of Solid and Liquid BW (Biological Warfare) Agents, Quarterly *12-M-3156*
Progress Report No. 10, period Sept. 4, 1962 - Dec. 4, 1962. G.R. Whitnah, Project Manager,
Approved by S.P. Jones, Aerospace Research, February 1963. 247 pages.

Sincerely

